

Accelerating Private Large Transformers Inference through Fine-grained Collaborative Computation

Yuntian Chen, Zhanyong Tang, Tianpei Lu, Bingsheng Zhang, Zhiying Shi, Zheng Wang

Abstract—Homomorphic encryption (HE) and secret sharing (SS) enable computations on encrypted data, providing significant privacy benefits for large transformer-based models (TBM) in sensitive sectors like medicine and finance. However, private TBM inference incurs significant costs due to the coarse-grained application of HE and SS. We present FASTLMPI, a new approach to accelerate private TBM inference through fine-grained computation optimization. Specifically, through the fine-grained co-design of homomorphic encryption and secret sharing, FASTLMPI achieves efficient protocols for matrix multiplication, SoftMax, LayerNorm, and GeLU. In addition, FASTLMPI introduces a precise segmented approximation technique for differentiable non-linear, improving its fitting accuracy while maintaining a low polynomial degree. Compared to solution BOLT (S&P'24), FASTLMPI shows a remarkable 54% to 64% decrease in runtime and an impressive 72.2% reduction in communication costs.

Index Terms—Secure multiparty computation, homomorphic encryption, privacy preserving, large transformer models.

I. INTRODUCTION

Deep learning models are often hosted in the cloud to provide inference services [1]. This provides a way for the service provider to protect the intellectual property of the trained model. However, sending user data to an untrusted cloud provider can raise privacy concerns as this can compromise data confidentiality [2].

Homomorphic encryption (HE) [3] and secure multi-party computation (MPC) [4] are two techniques for privacy-preserving deep learning inference. HE enables models to compute on encrypted user inputs and return encrypted results that are decrypted only by the user. MPC allows multiple parties to jointly compute functions on their private inputs by splitting data into shared pieces, ensuring no party has access to the full dataset or intermediate results, thereby maintaining privacy throughout the inference process.

Unfortunately, HE and MPC also have drawbacks, as HE can massively slow down model performance, while MPC introduces substantial communication overhead. Previous efforts have sought to combine HE and MPC by using HE for matrix multiplication - the dominant computation pattern in deep neural networks (DNNs) - and MPC for other DNN operations. This approach aims to leverage the strengths of both techniques. However, it still faces significant computational overhead, as matrix multiplication can account for over 90% of inference time in modern DNN architectures like Transformer-based models (TBMs) [5].

As a concrete example, Table I reports the results for applying BOLT [6]. The high volume of linear operations,

TABLE I: The performance percentage of each operator in BOLT under LAN network setting.

Operations	HE		SS	
	Linear	SoftMax	GeLU	LayerNorm
Runtime	74.5%	9.3%	8.1%	8.1%
Comm.	1.2%	40.7%	41.3%	16.8%

specifically matrix multiplications, is one of the primary contributors to inference latency. Non-linear operators, including SoftMax, GeLU, and LayerNorm, are major contributors to increased communication costs, especially in challenging network environments where they become the primary performance bottleneck. End-to-end inference experiments show that although BumbleBee [7] exhibits advantages in certain linear operations, FASTLMPI's superior performance in non-linear operations makes it more competitive overall.

The design of more practical private TBM inference is hindered by the following challenges:

- 1) **High inference latency:** The attention mechanism has significantly enhanced the learning and analysis capabilities of the model compared to traditional convolution. However, this comes at the cost of substantially increased computational complexity, demanding matrix multiplication operations with large dimensions of $128 \times 768 \times 64$ and $128 \times 768 \times 3072$. Large-scale matrix multiplication is a significant optimization problem. Computational efficiency under ciphertext is of particular concern. Most of the existing cryptographic protocols for private matrix multiplication rely on HE. While HE offers the benefit of concise communication cost, it requires time-consuming operation rotation, leading to poor inference efficiency. **The first challenge** is to design an efficient secure matrix multiplication protocol.
- 2) **High communication cost:** Compared to the ReLU non-linear functions commonly used in convolutional neural networks, TBM employs more sophisticated non-linear functions such as SoftMax within attention mechanisms, GeLU in feed-forward networks, and LayerNorm for normalization. These non-linear operations often rely on MPC techniques like secret sharing (SS) [8]. In BERT_{base}, the SoftMax function is invoked 2.36×10^6 times, requiring 300 rounds of interaction, resulting in a communication cost of 1447.65 MB. **The second challenge** is to design efficient protocols for

non-linear with low communication costs.

- 3) **High-degree, low-accuracy piecewise approximation:** A line of works [6], [7], [9], [10] typically uses the piecewise fitting method for non-linear e.g. GeLU, often with very similar segment endpoints. However, we found that the errors were huge at these endpoints, which was the primary reason for the decline in the accuracy of the approximation function. Moreover, the use of piecewise approximation necessitates higher-degree polynomials, thereby increasing computational complexity. For instance, Lu et.al [7], [10] use sixth-degree polynomials for piecewise approximation of the GeLU function.

The third challenge is to develop piecewise functions with higher precision while maintaining low-degree polynomial coefficients.

Based on the above analysis, we observe a pattern: existing private TBM inference solutions employ HE techniques to design secure matrix multiplication protocols for linear operators and SS techniques to design secure protocols for non-linear operators such as SoftMax, GeLU, and LayerNorm. In other words, after distinguishing between linear and non-linear operators at a high level, different cryptographic primitives are independently used to design secure protocols. While this classic strategy has effectively advanced the inference latency and communication costs of private TBM inference, the independent use of HE and SS is more likely to reveal the drawbacks of slow computation in HE and high communication costs in SS.

Motivated by this, we aim to provide a highly efficient and communication-friendly solution, called FASTLMPI, for private TBM inference. FASTLMPI integrates HE and SS at a finer granularity, proposing novel protocols that eliminate the high-level distinction between linear and nonlinear operations, such as Matmul-LayerNorm and Matmul-SoftMax. Rather than applying HE solely to Matmul and SS to SoftMax, LayerNorm, and GeLU, we break down these operator boundaries and choose between HE and SS at a more granular level. Specifically, the strategic integration of SS into HE-based Matmul protocol eliminates the computationally expensive rotation operation without increasing computational overhead. Moreover, using HE techniques in intermediate steps of non-linear leads to a substantial reduction in communication overhead. For example, in the exponential calculation, we can compute the exponential of additive SS, package intermediate results into SIMD-based HE ciphertexts, and perform ciphertext-plaintext addition to obtain the result, which is known to be more efficient than ciphertext-ciphertext multiplications [11] and we just need to introduce little acceptable communication costs. Compared to Cryptflow2 [12], which demands 117 rounds of interaction and incurs a communication cost of 592KB for the computation of the exponential of a 128×128 dimensional, our method only needs to send a single SIMD-based ciphertext (approximately 340KB).

Piecewise approximation of non-linear functions is another

focus of our work. The concavity, convexity, and curvature of a function are usually determined by inflection points, which are the points where the second derivative of the function is zero. At these points, the curvature of the function is usually small, indicating that the function tends to be smooth. Therefore, we select these special points as segment endpoints for function fitting, which can solve the problem of large errors at segment endpoints in traditional methods. An additional benefit is that piecewise functions have lower polynomial degrees. This approach applies to GeLU and can be extended to other differentiable non-linear functions such as the conventional activate function, e.g. Sigmoid, Tanh, and Mish.

To summarize, our contributions are as follows:

- 1) **Novel protocol based on fine-grained integration of HE and SS :** We propose new 2PC protocols, including secure matrix multiplication Π_{matmul} , secure Softmax Π_{softmax} , secure layerNorm Π_{ln} , and secure GeLU Π_{gelu} . Compared to BOLT, our protocols achieve $40\times$, $14\times$, $2\times$, and $2.2\times$ speedups, respectively. While reducing communication cost of Π_{softmax} , Π_{ln} and Π_{gelu} by $260\times$, $5.5\times$, and $3\times$, respectively.
- 2) **Better piecewise approximation for non-linear functions:** A novel piecewise approximation method is proposed for the differentiable nonlinear functions, offering enhanced accuracy with a lower polynomial degree. Such as Tanh uses polynomials of degree 4 to match the accuracy of BOLT, which uses polynomials of degree 5.
- 3) **End-to-end private inference performance improvement:** We implemented the end-to-end private TBM inference and conducted extensive experiments to evaluate the performance of our method thoroughly. FASTLMPI significantly reduces communication by about 50GB and end-to-end inference time by 2.2 to 24 minutes across various network environments. The code of FASTLMPI is available on the anonymous GitHub¹.

II. PRELIMINARIES

A. Notations

In this paper, we focus on 2PC setting $\mathcal{P} \in \{\mathcal{A}, \mathcal{B}\}$. We use $\mathbf{x} := \{x_0, \dots, x_{d_m-1}\} \in \mathbb{Q}^{d_m}$ to denote a vector of length m , and x_i represents the i -th element of the vector. $\mathbf{X} \in \mathbb{Q}^{d_m \times d_n}$ represents a matrix, where d_m denotes the number of rows, d_n denotes the number of columns, and x_{ij} represents the (i, j) -th entry of matrix \mathbf{X} . We use $[\mathbf{m}]_{\mathcal{P}}$ denotes the message encrypted by participant \mathcal{P} . $\langle m \rangle_{\mathcal{P}}$ and $\langle m \rangle_{\mathcal{P}}^B$ denote additive sharing and boolean sharing of m held by \mathcal{P} , respectively. We use \boxplus and \boxtimes to denote homomorphic addition and homomorphic multiplication computations. For plaintext, we denote the Hadamard product by \odot , element-wise addition by \oplus , matrix multiplication (or vector inner product)

¹<https://anonymous.4open.science/r/FASTLMPI>

² \mathbb{Q} represents the set of all rational numbers.

by \otimes , and XOR is denoted using the symbol \wedge . $\tilde{\mathbf{X}}$ denotes a rearrangement of matrix \mathbf{X} based on different requirements, while $\hat{\mathbf{X}}$ denotes a copy of the \mathbf{X} . \mathbb{Z}_p denotes prime fields (p is prime), and \mathbb{Z}_{2^k} denotes the ring. Given a real number \bar{x} , we use fixed-point encoding with s bit of precision, denotes $x = \lfloor \bar{x} \cdot 2^s \rfloor$.

B. TBM architecture

In most cases, TBM uses the decoder-only mode, exemplified by models such as BERT_{base}, as shown in Figure 1. The following section discusses the key operators of a single BERT_{base} block.

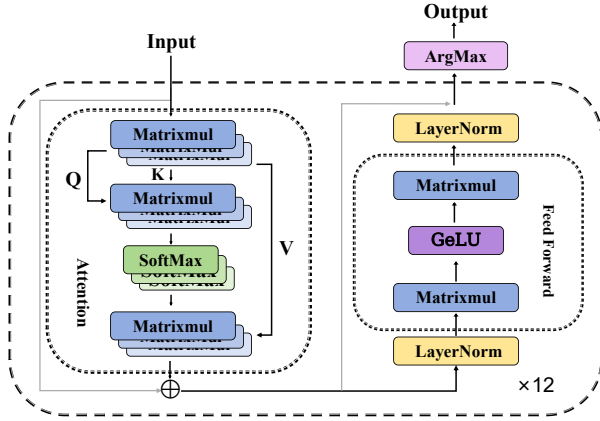


Fig. 1: The architecture of BERT_{base}.

1) *Attention Layer*: Given matrices \mathbf{Q} (query), \mathbf{K} (key), \mathbf{V} (value) in the latent represent, This attention layer can be formalized as Eq. (1) :

$$\text{Attention}(\mathbf{Q}, \mathbf{K}, \mathbf{V}) = \text{SoftMax} \left(\frac{\mathbf{Q} \otimes \mathbf{K}^T}{\sqrt{d_k}} \right) \mathbf{V} \quad (1)$$

where $\mathbf{Q}, \mathbf{K}, \mathbf{V} \in \mathbb{Q}^{d_s \times d_k}$. The SoftMax function applies to each row vector of a matrix. For a vector $\mathbf{x} \in \mathbb{Q}^{d_s}$. The SoftMax on \mathbf{x} returns a vector $\mathbf{y} \in \mathbb{Q}^{d_s}$ can be described as Eq. (2):

$$\mathbf{y} = \text{SoftMax}(x_i) = \frac{e^{x_i}}{\sum_{j=0}^{k-1} e^{x_j}} \quad (2)$$

The multi-head attention can be further extended by employing the attention mechanism. Considering h different attention mechanisms with weight matrices $\mathbf{W}_i^Q, \mathbf{W}_i^K, \mathbf{W}_i^V$ for $i = 1, \dots, h$, we have

$$\mathbf{h}_i = \text{Attention}(\mathbf{Q} \otimes \mathbf{W}_i^Q, \mathbf{K} \otimes \mathbf{W}_i^K, \mathbf{V} \otimes \mathbf{W}_i^V) \quad (3)$$

where $\mathbf{W}_i^Q, \mathbf{W}_i^K, \mathbf{W}_i^V \in \mathbb{Q}^{d_k \times d_m}$, and $\mathbf{h}_i \in \mathbb{Q}^{d_s \times d_m}$. Then, the multi-head attention can be formalized as Eq. (4):

$$\text{MH}(\mathbf{Q}, \mathbf{K}, \mathbf{V}) = (\mathbf{h}_1 || \mathbf{h}_2 || \dots || \mathbf{h}_h) \odot \mathbf{W}^O \quad (4)$$

where "||" denotes the horizontal concatenation of matrices, $\mathbf{W}^O \in \mathbb{Q}^{hd_k \times d_m}$, and $\text{MH}(\mathbf{Q}, \mathbf{K}, \mathbf{V}) \in \mathbb{Q}^{d_s \times d_m}$

2) *LayerNorm Layer*: Let $\mathbf{x} := (x_1, x_2, \dots, x_k)$ be a vector representation of an input of size d_k to normalization layers. LayerNorm re-centers and re-scales input $\mathbf{x} \in \mathbb{Q}^{d_k}$ as Eq.(5):

$$\text{LayerNorm}(x_i) = \gamma \cdot \frac{x_i - \mu}{\sigma} + \beta \quad (5)$$

where $\mu = \frac{1}{N} \sum_{i=1}^N x_i$, and $\sigma = \sqrt{\frac{1}{N} \sum_{i=1}^N (x_i - \mu)^2}$. μ and σ are the mean and standard deviation of \mathbf{x} .

3) *Feed-forward Layer (FFN)*: The FFN consists of two fully connected layers and is separated by a GeLU activation. Let $\mathbf{X} \in \mathbb{Q}^{d_s \times d_m}$ be an input, where d_s is the sequence length. The formula is as Eq. (6):

$$\text{FFN}(\mathbf{X}) = \text{GeLU}(\mathbf{X} \otimes \mathbf{W}^{F1} \oplus \mathbf{B}^{F1}) \otimes \mathbf{W}^{F2} \oplus \mathbf{B}^{F2} \quad (6)$$

where $\mathbf{W}^{F1} \in \mathbb{Q}^{d_m \times d_f}$, $\mathbf{W}^{F2} \in \mathbb{Q}^{d_m} \times d_f$ are the weight matrices and $\mathbf{B}^{F1} \in \mathbb{Q}^{d_f}$, $\mathbf{B}^{F2} \in \mathbb{Q}^{d_m}$ are the bias vectors for the two layers of FFN. GeLU is the Gaussian Error Linear Unit activation function, which returns a vector $\mathbf{y} \in \mathbb{Q}^{d_k}$ for the input vector $\mathbf{x} \in \mathbb{Q}^{d_k}$, as the Eq. (7):

$$\text{GeLU}(x_i) = x_i \cdot \Phi(x_i) = x_i \cdot \frac{1}{2} \left[1 + \text{erf} \left(\frac{x_i}{\sqrt{2}} \right) \right] \quad (7)$$

where $\Phi(x_i)$ is the standard Gaussian cumulative distribution function.

C. Threat Model

This work considers two-party computation secure against a semi-honest adversary [13]. The security is provided in simulation paradigm [14] against static and semi-honest probabilistic polynomial-time (PPT) adversary Adv. That is, the adversary Adv passively corrupts either \mathcal{A} or \mathcal{B} at the beginning of the protocol to learn something more than expected during interactions but honestly follows the protocol specification. The formal definition of the semi-honest security model is that for protocol Π (corresponding to the functionality \mathcal{F}), we assume that there is a simulation Sim can build a real world where the views (including all the intermediate values and outputs) of adversary Adv are computationally indistinguishable with the views in the real world:

$$\{ \text{View}_{\text{Adv}}^{\Pi}(\lambda, \langle x \rangle_{\mathcal{A}}, \langle x \rangle_{\mathcal{B}}), \text{output}^{\Pi}(\mathbf{y}) \} \stackrel{c}{\approx} \mathcal{S}(k, \{ \langle x \rangle_{\mathcal{P}}, \mathcal{F}(\langle x \rangle_{\mathcal{A}}, \langle x \rangle_{\mathcal{B}}) \}) \quad (8)$$

where λ is the secure parameter. $\text{View}_{\text{Adv}}^{\Pi}$ is the view of \mathcal{P} in the execution of Π on x , output^{Π} is the output of all parties. A detailed security proof of our proposed protocol is given in Appendix VIII.

D. Cryptographic Primitives

1) *Fully Homomorphic Encryption*: Fully Homomorphic Encryption (FHE) is first proposed by Rivest et al. [15]. We chose the Brakerski-Fan-Vercauteren (BFV) scheme [16], [17], whose security is based on the Ring Learning With Errors (RLWE) problem proposed by Lyubashevsky et al. [18]. The

BFV scheme has five algorithms, (**KeyGen**, **Encrypt**, **Decrypt**, **HAdd**, **HMult**, **Square**). **KeyGen** generates the keys used in the FHE scheme given the parameters chosen. **Encrypt** and **Decrypt** are the encryption and decryption algorithms respectively. **HAdd**, **HMult**, **Square** denote homomorphic addition, homomorphic multiplication operations and homomorphic squaring operations, respectively. A formal description with complete details can be found in [19]. BFV scheme supports packing into ciphertext in a single-instruction-multiple-data (SIMD) [20]. We adopted this technique to encrypt the messages.

2) *Secret Sharing Scheme*: Secret Sharing (SS) [21]: Allowing a set of 2 participants $\mathcal{P} \in \{\mathcal{A}, \mathcal{B}\}$ to share a piece of information in such a way that only authorized subsets of the participants can recover the secret.

We have the **Additive Scheme**: For every secret $s \in \mathbb{Z}_{2^k}$, an additive scheme satisfies $s = \langle s \rangle_{\mathcal{A}} + \langle s \rangle_{\mathcal{B}} \bmod 2^k$. When $k = 1$, the boolean secret sharing of s can be represented as $\langle s \rangle_{\mathcal{P}}^B$, satisfying $s = \langle s \rangle_{\mathcal{A}}^B \wedge \langle s \rangle_{\mathcal{B}}^B \bmod \mathbb{Z}_2$.

3) *Conversion between \mathbb{Z}_{2^k} and \mathbb{Z}_p* : FASTLMPI uses fixed-point number expression (Similar to [22], [23], [24]) and is based on the collaborative computation of HE and SS. It is worth noting that the HE is over \mathbb{Z}_p , while computation in SS is performed over \mathbb{Z}_{2^k} . We need to convert between \mathbb{Z}_p and \mathbb{Z}_{2^k} . In detail, converting from \mathbb{Z}_p to \mathbb{Z}_{2^k} requires comparison and a multiplexer. When converting from \mathbb{Z}_{2^k} to \mathbb{Z}_p , the probability that the sharing overflows is $\frac{|x|}{2^k}$. If x is small or the ring size is large enough, the conversion from \mathbb{Z}_{2^k} to \mathbb{Z}_p can be omitted without affecting the accuracy.

III. SYSTEM DESCRIPTION

In this section, we introduce the building blocks in FASTLMPI, which include four 2PC protocols: Secure Matrix Multiplication Π_{matmul} , secure Softmax Π_{softmax} , secure Layer-Norm Π_{ln} , fitting method of differentiable non-linear functions and secure GeLU Π_{gelu} . FASTLMPI is built in a 2-PC scenario where Alice (\mathcal{A}) represents the client and Bob (\mathcal{B}) represents the server. It relies on the fact that each party \mathcal{P} holds their data as input, and Alice and Bob can generate their private and public keys in the initial phase. FASTLMPI completes the protocol calculation when Alice and Bob interact to obtain the final privacy inference result.

A. Secure Matrix multiplication Π_{matmul}

This section details a secure matrix multiplication protocol. In the initial stage, party \mathcal{A} holds the input matrix $\mathbf{X} \in \mathbb{Z}_p^{d_m \times d_n}$, party \mathcal{B} holds the parameter $\mathbf{W}^I \in \mathbb{Z}_p^{d_n \times d_h}$, where $I \in \{Q, K, V\}$. In $\text{BERT}_{\text{base}}$, \mathbf{X} and \mathbf{W}^I can be packaged and directly implemented by SIMD-based homomorphic ciphertext-text multiplication to obtain $\mathbf{Q} \in \mathbb{Z}_p^{d_m \times d_h}$, $\mathbf{K} \in \mathbb{Z}_p^{d_m \times d_h}$ and $\mathbf{V} \in \mathbb{Z}_p^{d_m \times d_h}$, which are in SIMD ciphertext form. However, \mathbf{Q} , \mathbf{K} , and \mathbf{V} can be constructed in the form of additive secret sharing. \mathcal{B} generates the uniformly random $\mathbf{R} \in \mathbb{Z}_p^{d_m \times d_h}$ locally and constructs $\langle \mathbf{Q} \rangle_{\mathcal{A}} = \mathbf{Q} \boxplus \mathbf{R}$, then $\langle \mathbf{Q} \rangle_{\mathcal{B}} = \mathbf{R}$.

$\langle \mathbf{K} \rangle_{\mathcal{A}}$ and $\langle \mathbf{K} \rangle_{\mathcal{B}}$ can be obtained using the same way. Then $\mathbf{M} \in \mathbb{Z}_p^{d_m \times d_m} = \mathbf{Q} \otimes \mathbf{K}^T$ can be expressed as:

$$\mathbf{M} = \underbrace{\langle \mathbf{Q} \rangle_{\mathcal{A}} \otimes \langle \mathbf{K}^T \rangle_{\mathcal{A}}}_{\mathcal{A} \text{ can compute locally}} \oplus \underbrace{\langle \mathbf{Q} \rangle_{\mathcal{B}} \otimes \langle \mathbf{K}^T \rangle_{\mathcal{B}}}_{\mathcal{B} \text{ can compute locally}} \oplus \underbrace{\langle \mathbf{Q} \rangle_{\mathcal{B}} \otimes \langle \mathbf{K}^T \rangle_{\mathcal{A}}}_{\mathcal{A} \text{ and } \mathcal{B} \text{ compute interactively}} \oplus \underbrace{\langle \mathbf{Q} \rangle_{\mathcal{A}} \otimes \langle \mathbf{K}^T \rangle_{\mathcal{B}}}_{\mathcal{A} \text{ and } \mathcal{B} \text{ compute interactively}} \quad (9)$$

It's worth noting that we need to deal with the part of interactive computation such as $\mathbf{X} \otimes \mathbf{W}$, $\langle \mathbf{Q} \rangle_{\mathcal{A}} \otimes \langle \mathbf{K}^T \rangle_{\mathcal{B}}$ and $\langle \mathbf{Q} \rangle_{\mathcal{B}} \otimes \langle \mathbf{K}^T \rangle_{\mathcal{A}}$. In subsequent descriptions, we will uniformly describe the matrices involved in the interactive computation: Alice holds matrix $\mathbf{A} \in \mathbb{Z}_p^{d_m \times d_n}$, and Bob holds matrix $\mathbf{B} \in \mathbb{Z}_p^{d_n \times d_k}$. \mathbf{A} and \mathbf{B} as illustrated in Eq. (10).

$$\mathbf{A} = \left\{ \begin{array}{cccc} \boxed{a_{00} \ a_{01} \ \cdots \ a_{0n}} = \mathbf{A}_1 & & & \\ a_{10} \ a_{11} \ \cdots \ a_{1n} & & & \vdots \\ \vdots & & & \vdots \\ \boxed{a_{m0} \ a_{m1} \ \cdots \ a_{mn}} = \mathbf{A}_m & & & \end{array} \right\}, \mathbf{B} = \left\{ \begin{array}{cccc} b_{00} \ b_{01} \ \cdots \ b_{0k} & & & \\ b_{10} \ b_{11} \ \cdots \ b_{1k} & & & \\ \vdots & & & \vdots \\ b_{n0} \ b_{n1} \ \cdots \ b_{nk} & & & \end{array} \right\} \quad (10)$$

\mathbf{A} is first flattened row-wise to obtain \mathbf{A}_i , $i \in \{1, \dots, m\}$, which is then copied k times to form $\tilde{\mathbf{A}}$. Meanwhile \mathbf{B} copied m times form $\hat{\mathbf{B}}$. $\tilde{\mathbf{A}}$ and $\hat{\mathbf{B}}$ as shown in Eq. (11) and Eq. (12), respectively.

$$\tilde{\mathbf{A}} = [(\mathbf{A}_1^T \ \cdots \ \mathbf{A}_1^T)_{d_k} \ (\mathbf{A}_2^T \ \cdots \ \mathbf{A}_2^T)_{d_k} \ (\mathbf{A}_m^T \ \cdots \ \mathbf{A}_m^T)_{d_k}] \quad (11)$$

$$\hat{\mathbf{B}} = [(\mathbf{B} \ \mathbf{B} \ \cdots \ \mathbf{B})_{d_m}] \quad (12)$$

As \mathbf{A} is \mathcal{A} 's private data, it cannot be directly sent to \mathcal{B} . To preserve data confidentiality, we need to encrypt $\tilde{\mathbf{A}}$ and send $[\tilde{\mathbf{A}}]_{\mathcal{A}}$ to \mathcal{B} . \mathcal{B} computes $\sum_{i=0}^m ([\tilde{a}_{ij}]_{\mathcal{A}} \times \hat{b}_{ij})$ to get $[\mathbf{C}]_{\mathcal{A}}$, which is shown in Eq. (13).

$$[\mathbf{C}]_{\mathcal{A}} = \left\{ \begin{array}{cccc} [\tilde{a}_{00}]_{\mathcal{A}} \hat{b}_{00} & [\tilde{a}_{01}]_{\mathcal{A}} \hat{b}_{01} & \cdots & [\tilde{a}_{0(m \times k)}]_{\mathcal{A}} \hat{b}_{0(m \times k)} \\ & & \boxplus & \\ [\tilde{a}_{10}]_{\mathcal{A}} \hat{b}_{10} & [\tilde{a}_{11}]_{\mathcal{A}} \hat{b}_{11} & \cdots & [\tilde{a}_{1(m \times k)}]_{\mathcal{A}} \hat{b}_{1(m \times k)} \\ & & \boxplus & \\ \vdots & \vdots & \ddots & \vdots \\ & & \boxplus & \\ [\tilde{a}_{m0}]_{\mathcal{A}} \hat{b}_{m0} & [\tilde{a}_{m1}]_{\mathcal{A}} \hat{b}_{m1} & \cdots & [\tilde{a}_{m(m \times k)}]_{\mathcal{A}} \hat{b}_{m(m \times k)} \end{array} \right\} \quad (13)$$

Fig 2 shows a toy example with $\mathbf{A}^{3 \times 4}$ and $\mathbf{B}^{4 \times 2}$.

The matrix multiplication result obtained using protocol Π_{matmul} is a SIMD-based ciphertext without any wasted ciphertext slots. Compared with plaintext matrix multiplication, no additional multiplication operations are introduced. Employing the method mentioned earlier, the SIMD-based ciphertext $[\mathbf{C}]_{\mathcal{A}}$

³ T denotes the transpose of the matrix

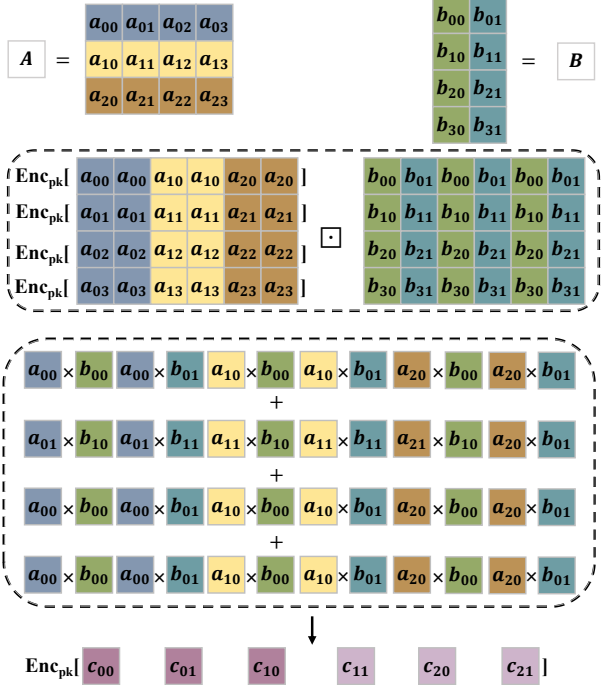


Fig. 2: A toy example of SIMD-based matrix multiplication

can be expressed as an additive secret sharing. This ensures that subsequent matrix multiplications can still be efficiently performed using homomorphic ciphertext-plaintext multiplication while remaining rotate-free. The protocol process is shown in Fig. 3. Now, $\langle \mathbf{Q} \rangle_{\mathcal{A}}, \langle \mathbf{K} \rangle_{\mathcal{A}}$ and $\langle \mathbf{Q} \rangle_{\mathcal{B}}, \langle \mathbf{K} \rangle_{\mathcal{B}}$ can be computed by $\Pi_{\text{matmul}}(\mathbf{X} \otimes \mathbf{W}_Q), \Pi_{\text{matmul}}(\mathbf{X} \otimes \mathbf{W}_K)$, respectively. Alice and Bob locally compute $\langle \mathbf{Q} \rangle_{\mathcal{A}} \odot \langle \mathbf{K} \rangle_{\mathcal{A}}$ and $\langle \mathbf{Q} \rangle_{\mathcal{B}} \odot \langle \mathbf{K} \rangle_{\mathcal{B}}$, respectively. Subsequently, Bob converts $\langle \mathbf{Q} \rangle_{\mathcal{B}} \odot \langle \mathbf{K} \rangle_{\mathcal{B}}$ to additive secret-sharing $\langle \mathbf{L} \rangle_{\mathcal{A}} = (\langle \mathbf{Q} \rangle_{\mathcal{B}} \odot \langle \mathbf{K} \rangle_{\mathcal{B}}) \ominus \mathbf{E}$ and $\langle \mathbf{L} \rangle_{\mathcal{B}} = \mathbf{E}$ (\mathbf{E} is a uniformly random matrix sampled from \mathbb{Z}_p , and has the same dimension with $\langle \mathbf{Q} \rangle_{\mathcal{B}} \odot \langle \mathbf{K} \rangle_{\mathcal{B}}$). Then Alice can obtain $\langle \mathbf{M} \rangle_{\mathcal{A}}$:

$$\langle \mathbf{M} \rangle_{\mathcal{A}} = (\langle \mathbf{Q} \rangle_{\mathcal{A}} \odot \langle \mathbf{K} \rangle_{\mathcal{A}}) \oplus \Pi_{\text{matmul}}(\langle \mathbf{Q} \rangle_{\mathcal{A}} \otimes \langle \mathbf{K} \rangle_{\mathcal{B}}) \oplus \Pi_{\text{matmul}}(\langle \mathbf{Q} \rangle_{\mathcal{B}} \boxtimes \langle \mathbf{K} \rangle_{\mathcal{A}}) \oplus \langle \mathbf{L} \rangle_{\mathcal{A}} \quad (14)$$

and Bob can obtain $\langle \mathbf{M} \rangle_{\mathcal{B}}$:

$$\langle \mathbf{M} \rangle_{\mathcal{B}} = \Pi_{\text{matmul}}(\langle \mathbf{Q} \rangle_{\mathcal{A}} \otimes \langle \mathbf{K} \rangle_{\mathcal{B}}) \oplus \Pi_{\text{matmul}}(\langle \mathbf{Q} \rangle_{\mathcal{B}} \boxtimes \langle \mathbf{K} \rangle_{\mathcal{A}}) \oplus \langle \mathbf{L} \rangle_{\mathcal{B}} \quad (15)$$

We opt for communication over the HE rotation. A single round of communication allows HE ciphertexts to be decomposed into the form of additive secret sharing, thus eliminating the need for rotation operations. Moreover, for specific matrix sizes, the communication cost is also acceptable.

Protocol Π_{matmul}

Initialization:

\mathcal{A} and \mathcal{B} generate each private key $sk_{\mathcal{A}}, sk_{\mathcal{B}}$ and public key $pk_{\mathcal{A}}, pk_{\mathcal{B}}$.

Private inputs:

\mathcal{A} : $\mathbf{A} \in \mathbb{Z}_p^{d_m \times d_n}$

\mathcal{B} : $\mathbf{B} \in \mathbb{Z}_p^{d_n \times d_h}$

Protocol:

1 \mathcal{A} : Flattens \mathbf{A} by rows and copies k times to obtain $\tilde{\mathbf{A}}$;

2 Encrypts each row of $\tilde{\mathbf{A}}$ by $pk_{\mathcal{A}}$ yields

3 SIMD-ciphertexts $\llbracket \tilde{\mathbf{A}} \rrbracket_{\mathcal{A}}$; Sends $\llbracket \tilde{\mathbf{A}} \rrbracket_{\mathcal{A}}$ to \mathcal{B} .

4 \mathcal{B} : Receives $\llbracket \tilde{\mathbf{A}} \rrbracket_{\mathcal{A}}$; Copies \mathbf{B} m times to get $\tilde{\mathbf{B}}$; Computes

5 $\llbracket \mathbf{C} \rrbracket_{\mathcal{A}} = \llbracket \tilde{\mathbf{A}} \rrbracket_{\mathcal{A}} \boxtimes \tilde{\mathbf{B}}$; Computes $\llbracket \mathbf{C} \rrbracket_{\mathcal{A}} = \sum_{i=0}^{m-1} \llbracket \mathbf{C}_i \rrbracket_{\mathcal{A}}$;

6 Generates uniformly random $\mathbf{R} \in \mathbb{Z}_p^{d_m \times d_h}$; Flattens \mathbf{R} to

7 obtain $\tilde{\mathbf{R}}$; Computes $\llbracket \langle \mathbf{C} \rangle_{\mathcal{A}} \rrbracket_{\mathcal{A}} = \llbracket \mathbf{C} \rrbracket_{\mathcal{A}} \boxtimes \tilde{\mathbf{R}}$; Sends

8 $\llbracket \langle \mathbf{C} \rangle_{\mathcal{A}} \rrbracket_{\mathcal{A}}$ to \mathcal{A} .

Private outputs:

9 \mathcal{A} : $\langle \mathbf{C} \rangle_{\mathcal{A}} = \mathbf{BFV.Decrypt}(sk_{\mathcal{A}}, \llbracket \langle \mathbf{C} \rangle_{\mathcal{A}} \rrbracket_{\mathcal{A}}) \in \mathbb{Z}_p$

10 \mathcal{B} : $\langle \mathbf{C} \rangle_{\mathcal{B}} = \tilde{\mathbf{R}} \in \mathbb{Z}_p$

1 $a_i \in \{0, 1, \dots, m\}$

Fig. 3: Secure matrix multiplication Π_{matmul}

B. Secure SoftMax Π_{softmax}

This subsection describes the secure SoftMax Π_{softmax} . As we know, mixing ring and prime shares will perform better. i.e., evaluate non-linear function over ring (\mathbb{Z}_{2^k}) shares, but switch to prime field (\mathbb{Z}_p) shares for arithmetic computations. Therefore, before computing function exp , we convert the shares from \mathbb{Z}_p to \mathbb{Z}_{2^k} . In subsequent calculations, it is assumed that the computational domain requires conversion, and we omit the description of the conversion process.

To describe the protocol implementation, assuming shares are already converted to \mathbb{Z}_{2^k} from \mathbb{Z}_p , \mathcal{A} and \mathcal{B} hold $\langle \mathbf{X} \rangle_{\mathcal{A}} \in \mathbb{Z}_{2^k}^{d_m \times d_m}$ and $\langle \mathbf{X} \rangle_{\mathcal{B}} \in \mathbb{Z}_{2^k}^{d_m \times d_m}$, respectively. We can directly call the Π_{rExp} protocol in SIRNN [25] to compute the exp function. \mathcal{A} and \mathcal{B} gets $\langle exp(\mathbf{X}) \rangle_{\mathcal{A}} \in \mathbb{Z}_p^{d_m \times d_m}$ and $\langle exp(\mathbf{X}) \rangle_{\mathcal{B}} \in \mathbb{Z}_p^{d_m \times d_m}$, respectively. Let \mathcal{B} flatten $\langle exp(\mathbf{X}) \rangle_{\mathcal{B}}$ row-wise, As shown in Eq. (16):

$$\langle exp(\mathbf{X}) \rangle_{\mathcal{B}} = \left\{ \begin{array}{l} \langle e^{x_{00}} \rangle_{\mathcal{B}} \quad \langle e^{x_{01}} \rangle_{\mathcal{B}} \quad \dots \quad \langle e^{x_{0k}} \rangle_{\mathcal{B}} = (\langle exp(\mathbf{X}) \rangle_{\mathcal{B}})_1 \\ \langle e^{x_{10}} \rangle_{\mathcal{B}} \quad \langle e^{x_{11}} \rangle_{\mathcal{B}} \quad \dots \quad \langle e^{x_{1k}} \rangle_{\mathcal{B}} = (\langle exp(\mathbf{X}) \rangle_{\mathcal{B}})_2 \\ \vdots \\ \langle e^{x_{n0}} \rangle_{\mathcal{B}} \quad \langle e^{x_{n1}} \rangle_{\mathcal{B}} \quad \dots \quad \langle e^{x_{nk}} \rangle_{\mathcal{B}} = (\langle exp(\mathbf{X}) \rangle_{\mathcal{B}})_m \end{array} \right. \quad (16)$$

we have:

$$\langle exp(\mathbf{X}) \rangle_{\mathcal{B}} = \left\{ (\langle exp(\mathbf{X}) \rangle_{\mathcal{B}})_1 \quad (\langle exp(\mathbf{X}) \rangle_{\mathcal{B}})_2 \quad \dots \quad (\langle exp(\mathbf{X}) \rangle_{\mathcal{B}})_m \right\} \quad (17)$$

Then \mathcal{B} encrypts $\langle exp(\mathbf{X}) \rangle_{\mathcal{B}}$, the result can be simply expressed as $\llbracket \langle \mathbf{E} \rangle_{\mathcal{B}} \rrbracket_{\mathcal{B}}$. Party \mathcal{B} sends the SIMD-based ciphertexts $\llbracket \langle \mathbf{E} \rangle_{\mathcal{B}} \rrbracket_{\mathcal{B}}$ to \mathcal{A} , which flattens $\langle exp(\mathbf{X}) \rangle_{\mathcal{A}}$ row-wise

similar to \mathcal{B} to get $\langle \widetilde{\text{exp}}(\mathbf{X}) \rangle_{\mathcal{A}}$. Next step \mathcal{A} computes $[\widetilde{\mathbf{E}}]_{\mathcal{B}} = [(\widetilde{\mathbf{E}})_{\mathcal{B}}]_{\mathcal{B}} \boxplus \langle \widetilde{\text{exp}}(\mathbf{X}) \rangle_{\mathcal{A}}$, which serves as the numerator of the Softmax function.

To compute the denominator, \mathcal{A} generates a uniformly random matrix $\mathbf{R} \in \mathbb{Z}_p^{d_m * d_h}$ and then flattens it row-wise using a similar pattern to obtain $\widetilde{\mathbf{R}}$. After that, \mathcal{A} computes $[\widetilde{\mathbf{E}}]_{\mathcal{B}} \boxplus \widetilde{\mathbf{R}}$ and the row sum of \mathbf{R} , and the resulting vector is denoted as $\mathbf{SR} = \sum_{i=0}^m (\mathbf{R})_i$. Subsequently, \mathcal{A} encrypts \mathbf{SR} , sends $[\widetilde{\mathbf{E}} \oplus \widetilde{\mathbf{R}}]_{\mathcal{B}}$ and $[\mathbf{SR}]_{\mathcal{A}}$ to \mathcal{B} . To achieve this, \mathcal{B} first decrypts the SIMD-based ciphertext $[\widetilde{\mathbf{E}} \oplus \widetilde{\mathbf{R}}]_{\mathcal{B}}$ by $sk_{\mathcal{B}}$ and restoring it to the original dimensions to get $(\mathbf{E} \oplus \mathbf{R}) \in \mathbb{Z}_p^{d_m * d_m}$. Next, the row sums of $\mathbf{E} \oplus \mathbf{R}$ are calculated, yielding $\sum_{i=0}^m (\mathbf{E}_i \oplus \mathbf{R}_i)$, which is expressed as Eq. (18):

$$\sum \mathbf{E} \oplus \sum \mathbf{R} = \left\{ \begin{array}{c} e_{00} + \dots + e_{0m} \\ e_{10} + \dots + e_{1m} \\ \vdots \\ e_{m0} + \dots + e_{mm} \end{array} \right\} \oplus \left\{ \begin{array}{c} r_{00} + \dots + r_{0m} \\ r_{10} + \dots + r_{1m} \\ \vdots \\ r_{m0} + \dots + r_{mm} \end{array} \right\} \quad (18)$$

The denominator $[\sum(\mathbf{E})]_{\mathcal{A}}$ is then obtained by subtracting the previously computed $[\mathbf{SR}]_{\mathcal{A}}$ from this sum.

Up to this point, we have obtained the numerator and denominator components of the SoftMax function, but direct division cannot be performed yet. Therefore, we construct $[\sum(\mathbf{E})]_{\mathcal{A}} \boxtimes \mathbf{v}$, where $\mathbf{v} \in \mathbb{Z}_p^{d_m}$ is another uniformly random vector generated by \mathcal{B} , and through an interactive round, obtain the modular inverse of the denominator at party \mathcal{B} . Coincidentally, the numerator $[\widetilde{\mathbf{E}}]_{\mathcal{B}}$ of the Softmax function is also SIMD-based ciphertext held by \mathcal{A} , allowing us to obtain the final result of Softmax easily.

Specifically, party \mathcal{B} first generates a uniformly random vector $\mathbf{v} \in \mathbb{Z}_p^{d_m}$. Simultaneously, \mathbf{v} is copied m times and tiled to obtain $\widehat{\mathbf{V}} \in \mathbb{Z}_p^{d_m * d_m}$. Then the encrypted $\widehat{\mathbf{V}}$ is sent to \mathcal{A} along with $[\sum(\mathbf{E})]_{\mathcal{A}} \boxtimes \mathbf{V}$. \mathcal{A} can decrypt $[\sum(\mathbf{E})]_{\mathcal{A}} \boxtimes \mathbf{V}$ and also copy $(\sum(\mathbf{E}) \boxtimes \mathbf{V})$ m times to obtain $(\sum(\widehat{\mathbf{E}}) \boxtimes \mathbf{V}) \in \mathbb{Z}_p^{d_m * d_m}$, and then compute the modular inverse $1/(\sum(\widehat{\mathbf{E}}) \boxtimes \mathbf{V})$. Next, by calculating $1/(\sum(\widehat{\mathbf{E}}) \boxtimes \mathbf{V})$ multiplied by $[\widehat{\mathbf{V}}]_{\mathcal{B}}$, we can obtain the modular inverse of the denominator of the Softmax function, $[1/\sum(\widehat{\mathbf{E}})]_{\mathcal{B}}$. Since the numerator $[\widetilde{\mathbf{E}}]_{\mathcal{B}}$ of the Softmax function is also held by \mathcal{A} , we can directly compute $[\widetilde{\mathbf{E}}]_{\mathcal{B}}$ multiplied by $[1/\sum(\widehat{\mathbf{E}})]_{\mathcal{B}}$ to obtain the final Softmax result $[\mathbf{Y}]_{\mathcal{B}}$. Finally, we can obtain the additive secret sharing $\langle \mathbf{Y} \rangle_{\mathcal{A}}$ and $\langle \mathbf{Y} \rangle_{\mathcal{B}}$ at partys \mathcal{A} and \mathcal{B} respectively, by adopting a method similar to that used in Π_{matmul} . The specific steps of the protocol are shown in Fig. 4. To facilitate understanding, a 3×3 matrix example for Softmax calculation is provided in Fig. 13 of Appendix IX-E.

C. secure LayerNorm Π_{ln}

This section describes the secure LayerNorm Π_{ln} . Eq. (5) presents the LayerNorm function.

Protocol Π_{softmax}

Initialization:

\mathcal{A} and \mathcal{B} generate each private key $sk_{\mathcal{A}}, sk_{\mathcal{B}}$ and public key $pk_{\mathcal{A}}, pk_{\mathcal{B}}$.

Private inputs:^a

\mathcal{A} : $\langle \mathbf{X} \rangle_{\mathcal{A}} \in \mathbb{Z}_{2k}^{d_m * d_m}$

\mathcal{B} : $\langle \mathbf{X} \rangle_{\mathcal{B}} \in \mathbb{Z}_{2k}^{d_m * d_m}$

Protocol:

\mathcal{P}^b : Participants \mathcal{A} and \mathcal{B} do the same as follow:

$$\langle \text{exp}(\mathbf{X}) \rangle_{\mathcal{P}} = \Pi_{\text{Exp}}(\langle \mathbf{X} \rangle_{\mathcal{P}})$$

\mathcal{B} : Flattens $\langle \text{exp}(\mathbf{X}) \rangle_{\mathcal{B}}$ row-wise to get $\langle \widetilde{\text{exp}}(\mathbf{X}) \rangle_{\mathcal{B}}$; Encrypts $\langle \widetilde{\text{exp}}(\mathbf{X}) \rangle_{\mathcal{B}}$ by $pk_{\mathcal{A}}$ yields $[(\widetilde{\text{exp}}(\mathbf{X}))_{\mathcal{B}}]_{\mathcal{B}}$ (simply expressed as $[(\mathbf{E})_{\mathcal{B}}]_{\mathcal{B}}$); Sends $[(\mathbf{E})_{\mathcal{B}}]_{\mathcal{B}}$ to \mathcal{A} .

\mathcal{A} : Receives $[(\mathbf{E})_{\mathcal{B}}]_{\mathcal{B}}$; Flattens $\langle \text{exp}(\mathbf{X}) \rangle_{\mathcal{A}}$ row-wise to get $\langle \widetilde{\text{exp}}(\mathbf{X}) \rangle_{\mathcal{A}}$; Computes $[\widetilde{\mathbf{E}}]_{\mathcal{B}} = [(\mathbf{E})_{\mathcal{B}}]_{\mathcal{B}} \boxplus \langle \widetilde{\text{exp}}(\mathbf{X}) \rangle_{\mathcal{A}}$; Generates a uniformly random matrix $\mathbf{R} \in \mathbb{Z}_p^{d_m * d_m}$; Computes $[\widetilde{\mathbf{E}}]_{\mathcal{B}} \boxplus \mathbf{R}$ and $\mathbf{SR} = \sum_{i=0}^m (\mathbf{R})_i$; Encrypts \mathbf{SR} ; Sends set $S_1 = \{[\widetilde{\mathbf{E}} \oplus \mathbf{R}]_{\mathcal{B}}, [\mathbf{SR}]_{\mathcal{A}}\}$ to \mathcal{B} .

\mathcal{B} : Receives S_1 from \mathcal{A} ; Decrypts $[\widetilde{\mathbf{E}} \oplus \mathbf{R}]_{\mathcal{B}}$ by $sk_{\mathcal{B}}$ yields $\widetilde{\mathbf{E}} \oplus \mathbf{R}$; Computes $[\sum(\mathbf{E})]_{\mathcal{A}} = \sum_{i=0}^m (\mathbf{E}_i + \mathbf{R}_i) \boxminus ([\mathbf{SR}]_{\mathcal{A}})$; Generates a uniformly random vector $\mathbf{v} \in \mathbb{Z}_p^{d_m}$; Computes $[\sum(\mathbf{E})]_{\mathcal{A}} \boxtimes \mathbf{v}$; \mathbf{v} is copied m times to get $\widehat{\mathbf{V}}$; Encrypts $\widehat{\mathbf{V}}$; Sends set $S_2 = \{[\sum(\mathbf{E}) \boxtimes \mathbf{v}]_{\mathcal{A}}, [\widehat{\mathbf{V}}]_{\mathcal{B}}\}$ to \mathcal{A} .

\mathcal{A} : Receives S_2 from \mathcal{B} ; Decrypts $[\sum(\mathbf{E}) \boxtimes \mathbf{v}]_{\mathcal{A}}$; Copies $(\sum(\mathbf{E}) \boxtimes \mathbf{v})$ also m times to get $(\sum(\widehat{\mathbf{E}}) \boxtimes \mathbf{V})$; Computes the modular inverse $1/(\sum(\widehat{\mathbf{E}}) \boxtimes \mathbf{V})$; Computes $[1/\sum(\widehat{\mathbf{E}})]_{\mathcal{B}} = 1/(\sum(\widehat{\mathbf{E}}) \boxtimes \mathbf{V}) \boxtimes [\widehat{\mathbf{V}}]_{\mathcal{B}}$; Computes $[\mathbf{Y}]_{\mathcal{B}} = [\widetilde{\mathbf{E}}]_{\mathcal{B}} \boxtimes [1/\sum(\widehat{\mathbf{E}})]_{\mathcal{B}}$; Generates a uniformly random matrix $\mathbf{M} \in \mathbb{Z}_p^{d_m * d_m}$; Flattens \mathbf{M} row-wise to get $\widetilde{\mathbf{M}}$; Computes $[(\mathbf{Y})_{\mathcal{B}}]_{\mathcal{B}} = [\mathbf{Y}]_{\mathcal{B}} \boxminus \widetilde{\mathbf{M}}$; Sends $[(\mathbf{Y})_{\mathcal{B}}]_{\mathcal{B}}$ to \mathcal{B} .

\mathcal{B} : Receives $[(\mathbf{Y})_{\mathcal{B}}]_{\mathcal{B}}$.

Private outputs:

\mathcal{A} : $\langle \mathbf{Y} \rangle_{\mathcal{A}} = \mathbf{M} \in \mathbb{Z}_p$

\mathcal{B} : $\langle \mathbf{Y} \rangle_{\mathcal{B}} = \text{BFV.Decrypt}(sk_{\mathcal{B}}, [(\mathbf{Y})_{\mathcal{B}}]_{\mathcal{B}}) \in \mathbb{GF}(p)$

^aBefore calculating function exp , the share is transferred from the prime field \mathbb{Z}_p to Ring \mathbb{Z}_{2k} , and after calculating exp , the share is transferred from \mathbb{Z}_{2k} to \mathbb{Z}_p .

^bSince \mathcal{A} and \mathcal{B} follow the same computation steps

Fig. 4: Secure softmax Π_{softmax}

Given a matrix $\mathbf{X} \in \mathbb{Z}_p^{d_m * d_n}$, x_{ij} is the element at the (i, j) position. Equivalently, LayerNorm can be expressed as (19):

$$\text{LayerNorm}(x_{ij}) = \gamma \sqrt{n} \odot \frac{a_{ij}}{\sqrt{\sum_{j=0}^n a_{ij}^2}} \oplus \beta \quad (19)$$

where $a_{ij} = nx_{ij} - n\mu_i = nx_{ij} - \sum_{j=0}^n x_{ij}$. Then it can be inferred that \mathbf{A} , and shown as:

$$\mathbf{A} = \begin{bmatrix} \mathbf{A}_1 \\ \mathbf{A}_2 \\ \vdots \\ \mathbf{A}_m \end{bmatrix}, \quad \mathbf{A}_i^T = \begin{bmatrix} a_{i1} \\ a_{i2} \\ \vdots \\ a_{in} \end{bmatrix} = \begin{bmatrix} (n-1)x_{i1} - x_{i2} - \dots - x_{in} \\ -x_{i1} + (n-1)x_{i2} - \dots - x_{in} \\ \vdots \\ -x_{i1} - x_{i2} - \dots + (n-1)x_{in} \end{bmatrix} \quad (20)$$

Consequently, the computation of a_{ij} in Eq. (19) can be readily computed locally and represented as a secret-sharing $\langle \mathbf{A} \rangle_{\mathcal{P}} \in \mathbb{Z}_{2k}^{d_m * d_n}$, $\mathcal{P} \in \{\mathcal{A}, \mathcal{B}\}$. The primary bottleneck lies

in the evaluation of the denominator $\sqrt{\sum_{j=0}^n a_{ij}^2}$. Specifically, after parties \mathcal{A} and \mathcal{B} obtain $\langle \mathbf{A} \rangle_{\mathcal{A}}$ and $\langle \mathbf{A} \rangle_{\mathcal{B}}$ respectively, they can flatten the secret sharing row-wise to form $\langle \tilde{\mathbf{A}} \rangle_{\mathcal{A}}$ and $\langle \tilde{\mathbf{A}} \rangle_{\mathcal{B}}$. This is convenient for encrypting the ciphertexts to the SIMD form. Subsequently, \mathcal{B} encrypts $\langle \tilde{\mathbf{A}} \rangle_{\mathcal{B}}$ and send $\llbracket \langle \tilde{\mathbf{A}} \rangle_{\mathcal{B}} \rrbracket_{\mathcal{B}}$ to \mathcal{A} . Party \mathcal{A} then sum $\langle \tilde{\mathbf{A}} \rangle_{\mathcal{A}}$ and $\llbracket \langle \tilde{\mathbf{A}} \rangle_{\mathcal{B}} \rrbracket_{\mathcal{B}}$ to obtain $\llbracket \mathbf{A} \rrbracket_{\mathcal{B}}$. Given the **BFV.square** operation, which is more than twice as efficient as the multiplication operation for two ciphertexts, so we employ **BFV.square** to efficiently compute $\llbracket \mathbf{A}^2 \rrbracket_{\mathcal{B}}$. At this point, a direct summation is not feasible. \mathcal{A} generates a uniformly random vector $\mathbf{R} \in \mathbb{Z}_p^{d_m * d_n}$ and computes $\llbracket \tilde{\mathbf{A}}^2 \rrbracket_{\mathcal{B}} \boxplus \mathbf{R}$, as outlined in Eq. (21):

$$\llbracket \tilde{\mathbf{A}}^2 \oplus \mathbf{R} \rrbracket_{\mathcal{B}} = \left\{ \begin{array}{cccc} \llbracket \tilde{\mathbf{A}}_1^2 \rrbracket_{\mathcal{B}} & \llbracket \tilde{\mathbf{A}}_2^2 \rrbracket_{\mathcal{B}} & \cdots & \llbracket \tilde{\mathbf{A}}_m^2 \rrbracket_{\mathcal{B}} \\ \boxplus & \boxplus & \cdots & \boxplus \\ \mathbf{R}_1 & \mathbf{R}_2 & \cdots & \mathbf{R}_m \end{array} \right\} \quad (21)$$

where \mathbf{R}_i , $i \in \{1, 2, \dots, m\}$ denotes the i -th row of matrix \mathbf{R} . While $\llbracket \tilde{\mathbf{A}}^2 \oplus \mathbf{R} \rrbracket_{\mathcal{B}}$ can be directly sent to \mathcal{B} , who can compute the row sum after decryption. However, \mathcal{B} can not eliminate \mathbf{R} directly. There, we let \mathcal{A} compute the row sum of \mathbf{R} , obtaining Eq. (22):

$$\mathbf{SR} = [\sum_{j=0}^n r_{1j} \quad \sum_{j=0}^n r_{2j} \quad \cdots \quad \sum_{j=0}^n r_{mj}] \quad (22)$$

Then, \mathcal{A} encrypts $\mathbf{SR} \in \mathbb{Z}_p^{d_m}$ and sends $\llbracket \mathbf{SR} \rrbracket_{\mathcal{A}}$ to \mathcal{B} . Next step, \mathcal{B} can compute the row sum like (18) after decrypts $\llbracket \tilde{\mathbf{A}}^2 \oplus \mathbf{R} \rrbracket_{\mathcal{B}}$, and obtain $\sum_{j=0}^n \tilde{a}_{ij}^2 \oplus \mathbf{SR}$ as Eq. (23):

$$\sum_{j=0}^n \tilde{a}_{ij}^2 \oplus \sum_{j=0}^n r_{ij} = \left\{ \begin{array}{cccc} \sum_{j=0}^n \tilde{a}_{1j}^2 & \sum_{j=0}^n \tilde{a}_{2j}^2 & \cdots & \sum_{j=0}^n \tilde{a}_{mj}^2 \\ \boxplus & \boxplus & \cdots & \boxplus \\ \sum_{j=0}^n r_{1j} & \sum_{j=0}^n r_{2j} & \cdots & \sum_{j=0}^n r_{mj} \end{array} \right\} \quad (23)$$

By subtracting $\llbracket \mathbf{SR} \rrbracket_{\mathcal{A}}$ from $\sum_{j=0}^n \tilde{a}_{ij}^2 \oplus \mathbf{SR}$, \mathcal{B} can subsequently obtain the sum of squares $\sum_{j=0}^n \tilde{a}_{ij}^2$ of $\llbracket \tilde{\mathbf{A}}^2 \rrbracket_{\mathcal{B}}$, abbreviated as $\llbracket \mathbf{SA}^2 \rrbracket_{\mathcal{A}}$.

To proceed, the square root is calculated. \mathcal{B} begins by generating a uniformly random vector $\mathbf{v} \in \mathbb{Z}_p^{d_m}$, which can be viewed as an additive sharing held by \mathcal{B} , denoted as $\langle \mathbf{K} \rangle_{\mathcal{B}} = \mathbf{v}$. \mathcal{B} also can form $\llbracket \mathbf{SA}^2 \rrbracket_{\mathcal{A}} \boxminus \mathbf{v}$, which is sent to \mathcal{A} . \mathcal{A} decrypts this to obtain $\langle \mathbf{K} \rangle_{\mathcal{A}} = (\mathbf{SA}^2 \ominus \mathbf{v}) \in \mathbb{Z}_p^{d_m}$. With $\langle \mathbf{K} \rangle_{\mathcal{A}}$ and $\langle \mathbf{K} \rangle_{\mathcal{B}}$ constituting additive secret shares over \mathbb{Z}_p , a conversion to the ring \mathbb{Z}_{2^k} is undertaken before computing the square root. At this point, \mathcal{A} and \mathcal{B} can invoke Π_{invsqrt} ⁴ to get the secret sharing $\langle 1/\sqrt{\mathbf{K}} \rangle_{\mathcal{A}}$ and $\langle 1/\sqrt{\mathbf{K}} \rangle_{\mathcal{B}}$, respectively.

Given the preceding computation, the party \mathcal{A} , holds the ciphertext $\llbracket \tilde{\mathbf{A}} \rrbracket_{\mathcal{B}}$. Consequently, we let party \mathcal{B} copy $\langle 1/\sqrt{\mathbf{K}} \rangle_{\mathcal{B}}$ n times and encrypt the additive sharing $\langle 1/\sqrt{\mathbf{K}} \rangle_{\mathcal{B}} \in \mathbb{Z}_p^{d_m * d_n}$ and send it to \mathcal{A} . Then party \mathcal{A} also copy $\langle 1/\sqrt{\mathbf{K}} \rangle_{\mathcal{A}}$ n times

and calculates $\llbracket 1/\sqrt{\mathbf{K}} \rrbracket_{\mathcal{B}} = \langle 1/\sqrt{\mathbf{K}} \rangle_{\mathcal{A}} \boxplus \llbracket \langle 1/\sqrt{\mathbf{K}} \rangle_{\mathcal{B}} \rrbracket_{\mathcal{B}}$. Now, \mathcal{A} can directly compute:

$$\llbracket \frac{a_i}{\sqrt{\sum_{j=0}^n a_{ij}^2}} \rrbracket_{\mathcal{B}} = \llbracket \tilde{\mathbf{A}} \rrbracket_{\mathcal{B}} \boxtimes \left(\llbracket 1/\sqrt{\mathbf{K}} \rrbracket_{\mathcal{B}} \right) \quad (24)$$

Protocol Π_{In}

Initialization:

\mathcal{A} and \mathcal{B} generate each private key $sk_{\mathcal{A}}, sk_{\mathcal{B}}$ and public key $pk_{\mathcal{A}}, pk_{\mathcal{B}}$.

Private inputs:

\mathcal{A} : $\langle \mathbf{X} \rangle_{\mathcal{A}} \in \mathbb{Z}_{2^k}^{d_m * d_n}$

\mathcal{B} : $\langle \mathbf{X} \rangle_{\mathcal{B}} \in \mathbb{Z}_{2^k}^{d_m * d_n}$, parameter $\gamma \in \mathbb{Z}_p^{d_m}$, $\beta \in \mathbb{Z}_p^{d_m}$

Protocol:

- 1 \mathcal{B} : Computes $\langle \mathbf{A} \rangle_{\mathcal{B}}$; Flatten $\langle \mathbf{A} \rangle_{\mathcal{B}}$ row-wise to get $\langle \tilde{\mathbf{A}} \rangle_{\mathcal{B}}$;
- 2 Encrypts $\langle \tilde{\mathbf{A}} \rangle_{\mathcal{B}}$ through $pk_{\mathcal{B}}$ to obtain $\llbracket \langle \tilde{\mathbf{A}} \rangle_{\mathcal{B}} \rrbracket_{\mathcal{B}}$; Sends
- 3 $\llbracket \langle \tilde{\mathbf{A}} \rangle_{\mathcal{B}} \rrbracket_{\mathcal{B}}$ to \mathcal{A} .
- 4 \mathcal{A} : Receives $\llbracket \langle \tilde{\mathbf{A}} \rangle_{\mathcal{B}} \rrbracket_{\mathcal{B}}$; Computes $\langle \mathbf{A} \rangle_{\mathcal{A}}$; Flattens it row-wise to
- 5 get $\langle \tilde{\mathbf{A}} \rangle_{\mathcal{A}}$; Computes $\llbracket \tilde{\mathbf{A}} \rrbracket_{\mathcal{B}} = \langle \tilde{\mathbf{A}} \rangle_{\mathcal{A}} \boxplus \llbracket \langle \tilde{\mathbf{A}} \rangle_{\mathcal{B}} \rrbracket_{\mathcal{B}}$; Calls
- 6 **BFV.square** a to get $\llbracket \langle \tilde{\mathbf{A}}^2 \rangle_{\mathcal{B}} \rrbracket_{\mathcal{B}}$; Generates a uniformly random
- 7 matrix $\mathbf{R} \in \mathbb{Z}_{2^k}^{d_m * d_n}$; Computes the sum of each row to get
- 8 $\mathbf{SR} \in \mathbb{Z}_p^{d_m}$, $\llbracket \mathbf{A}^2 \rrbracket_{\mathcal{B}} \boxplus \mathbf{R}$; Encrypts \mathbf{SR} ; Sends set $S_1 =$
- 9 $\{\llbracket \tilde{\mathbf{A}}^2 \oplus \mathbf{R} \rrbracket_{\mathcal{B}}, \llbracket \mathbf{SR} \rrbracket_{\mathcal{A}}\}$ to \mathcal{B} .
- 10 \mathcal{B} : Receives S_1 ; Decrypts $\{\llbracket \tilde{\mathbf{A}}^2 \oplus \mathbf{R} \rrbracket_{\mathcal{B}}, \llbracket \mathbf{SR} \rrbracket_{\mathcal{A}}\}$; Computes row sum of
- 11 $(\tilde{\mathbf{A}}^2 \oplus \mathbf{R})$ to get $\sum_{j=0}^n \tilde{a}_{ij}^2 \oplus \mathbf{SR}$; Computes $\sum_{j=0}^n \tilde{a}_{ij}^2 \oplus \mathbf{SR}$
- 12 $\boxminus \llbracket \mathbf{SR} \rrbracket_{\mathcal{A}}$ to get $\llbracket \sum_{j=0}^n \tilde{a}_{ij}^2 \rrbracket_{\mathcal{A}}$; Generates uniformly random
- 13 vector $\mathbf{v} \in \mathbb{Z}_p^{d_m}$; Computes $\llbracket \sum_{j=0}^n \tilde{a}_{ij}^2 \rrbracket_{\mathcal{A}} \boxminus \mathbf{v}$; \mathcal{B} has
- 14 $\langle \mathbf{K} \rangle_{\mathcal{B}} = \mathbf{v}$; Calls Π_{invsqrt} to get $\langle 1/\sqrt{\mathbf{K}} \rangle_{\mathcal{B}}$, copies $\langle 1/\sqrt{\mathbf{K}} \rangle_{\mathcal{B}}$
- 15 n times and encrypts $\langle 1/\sqrt{\mathbf{K}} \rangle_{\mathcal{B}} \in \mathbb{Z}_p^{d_m * d_n}$; Sends set $S_2 = \{$
- 16 $\llbracket \langle 1/\sqrt{\mathbf{K}} \rangle_{\mathcal{B}} \rrbracket_{\mathcal{B}}, \{\llbracket \sum_{j=0}^n \tilde{a}_{ij}^2 \rrbracket_{\mathcal{A}} \boxminus \mathbf{v} \rrbracket_{\mathcal{A}}\}$, to \mathcal{A} .
- 17 \mathcal{A} : Receives S_2 ; Decrypts $\llbracket \sum_{j=0}^n \tilde{a}_{ij}^2 \boxminus \mathbf{v} \rrbracket_{\mathcal{A}}$ to get
- 18 $\langle \mathbf{K} \rangle_{\mathcal{A}} = \sum_{j=0}^n \tilde{a}_{ij}^2 \ominus \mathbf{v}$; Calls Π_{invsqrt} to get $\langle 1/\mathbf{K} \rangle_{\mathcal{A}}$, also
- 19 copies it n times to get $\langle 1/\sqrt{\mathbf{K}} \rangle_{\mathcal{A}}$; Computes
- 20 $\llbracket 1/\sqrt{\mathbf{K}} \rrbracket_{\mathcal{B}} = \langle 1/\sqrt{\mathbf{K}} \rangle_{\mathcal{A}} \boxplus \llbracket \langle 1/\sqrt{\mathbf{K}} \rangle_{\mathcal{B}} \rrbracket_{\mathcal{B}}$ and $\llbracket \frac{a_i}{\sqrt{\sum_{j=0}^n a_{ij}^2}} \rrbracket_{\mathcal{B}} =$
- 21 $\llbracket \tilde{\mathbf{A}} \rrbracket_{\mathcal{B}} \boxtimes \llbracket 1/\sqrt{\mathbf{K}} \rrbracket_{\mathcal{B}}$; Generates a uniformly random matrix
- 22 $\mathbf{S} \in \mathbb{Z}_p^{d_m * d_n}$; Flattens \mathbf{S} row-wise to get $\tilde{\mathbf{S}}$; Computes
- 23 $\llbracket \frac{a_i}{\sqrt{\sum_{j=0}^n a_{ij}^2}} \rrbracket_{\mathcal{B}} \boxtimes \tilde{\mathbf{S}}$; Sends set $S_3 = \{\llbracket \frac{a_i}{\sqrt{\sum_{j=0}^n a_{ij}^2}} \boxtimes \tilde{\mathbf{S}} \rrbracket_{\mathcal{B}}, \llbracket \tilde{\mathbf{S}} \rrbracket_{\mathcal{A}}\}$ to
- 24 \mathcal{B} .
- 25 \mathcal{B} : Receives S_3 ; Decrypts $\llbracket \frac{a_i}{\sqrt{\sum_{j=0}^n a_{ij}^2}} \boxtimes \tilde{\mathbf{S}} \rrbracket_{\mathcal{B}}$ to get $\frac{a_i}{\sqrt{\sum_{j=0}^n a_{ij}^2}} \ominus \tilde{\mathbf{S}}$;
- 26 Computes $\llbracket \frac{a_i}{\sqrt{\sum_{j=0}^n a_{ij}^2}} \rrbracket_{\mathcal{A}} = \frac{a_i}{\sqrt{\sum_{j=0}^n a_{ij}^2}} \ominus \tilde{\mathbf{S}} \boxplus \llbracket \tilde{\mathbf{S}} \rrbracket_{\mathcal{A}}$; Computes
- 27 $\llbracket \mathbf{Y} \rrbracket_{\mathcal{A}} = \gamma \odot \sqrt{n} \boxtimes \llbracket \frac{a_i}{\sqrt{\sum_{j=0}^n a_{ij}^2}} \rrbracket_{\mathcal{A}} \boxplus \beta$. Generates a uniformly
- 28 random matrix $\mathbf{M} \in \mathbb{Z}_p^{d_m * d_n}$. Computes $\llbracket \mathbf{Y} \rrbracket_{\mathcal{A}} \boxplus \mathbf{M}$ and Sends
- 29 to \mathcal{A} .
- 30 \mathcal{A} : Receives $\llbracket \mathbf{Y} \rrbracket_{\mathcal{A}} \boxplus \mathbf{M}$.

Private outputs:

\mathcal{A} : $\langle \mathbf{Y} \rangle_{\mathcal{A}} = \mathbf{BFV.Decrypt}(sk_{\mathcal{A}}, \llbracket \mathbf{Y} \rrbracket_{\mathcal{A}} \boxplus \mathbf{M})$

\mathcal{B} : $\langle \mathbf{Y} \rangle_{\mathcal{B}} = \mathbf{M}$

⁴this function from SEAL [26]

Fig. 5: Protocol secure layernorm Π_{In}

The parameters γ and β of LayerNorm are held by party \mathcal{B} . Therefore, \mathcal{A} generates a uniformly random matrix $\mathbf{S} \in \mathbb{Z}_p^{d_m * d_n}$, flattens it row-wise to get $\tilde{\mathbf{S}}$ and calculates $\llbracket \frac{a_i}{\sqrt{\sum_{j=0}^n a_{ij}^2}} \rrbracket_{\mathcal{B}} \boxtimes \tilde{\mathbf{S}}$ and encrypts $\tilde{\mathbf{S}}$. These SIMD-based ciphertexts

⁴The secure inverse square root protocol Π_{invsqrt} , sourced from the SCI_{lib} [25]

are then sent to \mathcal{B} , which decrypts $\llbracket \frac{a_i}{\sqrt{\sum^n a_i^2}} \ominus \tilde{\mathbf{S}} \rrbracket_{\mathcal{B}}$ and add $\llbracket \tilde{\mathbf{S}} \rrbracket_{\mathcal{A}}$ to obtain $\llbracket \frac{a_i}{\sqrt{\sum^n a_i^2}} \rrbracket_{\mathcal{A}}$. Finally, \mathcal{B} can compute the LayerNorm output $\llbracket Y \rrbracket_{\mathcal{A}} = \gamma \sqrt{n} \square \llbracket \frac{a_i}{\sqrt{\sum^n a_i^2}} \rrbracket_{\mathcal{A}} \boxplus \beta$, where $\gamma \in \mathbb{Z}_p^{d_m}$ $\beta \in \mathbb{Z}_p^{d_m}$.

Subsequently, through a single round of communication, \mathcal{B} can distribute $\langle \mathbf{Y} \rangle_{\mathcal{A}}$ and $\langle \mathbf{Y} \rangle_{\mathcal{B}}$ to \mathcal{A} and \mathcal{B} , respectively. The specific process of Π_{ln} is shown in Fig. 5. A 3×3 matrix is presented as an illustrative example to demonstrate the calculation of LayerNorm. Specific details can be found in Fig. 14 of Appendix IX-E.

D. Fitting of differentiable non-linear functions

This section introduces piecewise approximation of non-linear functions, with a focus on GeLU as a specific example due to its application in subsequent protocols. Due to the incompatibility of cryptographic techniques with non-linear functions, existing methods usually approximate the GeLU function in segments to achieve secure computation, but this approximation often leads to computational errors [6], [7]. By analyzing different approaches, we found that these errors usually stem from the vicinity of the boundary points of the intervals. This indicates that choosing more reasonable boundary points is necessary and can greatly reduce the error. Thus, starting from the nature of the function itself, we provide a high-precision approximate function for the GeLU.

As is well known, the second derivative of a function can determine the inflection points (or concavity) of the function within a given interval, indicating the curvature of the function in that interval. Inflection points, where the second derivative is zero, are special points that distinguish between concave and convex regions. Typically, the function's curve changes relatively smoothly at these points, meaning the function fluctuates relatively little. Therefore, we select inflection points as the endpoints of our piecewise function intervals to minimize the impact of piecewise approximation on function accuracy. Based on this, we approximate and replace the function. If no inflection points exist, we can calculate the third derivative. The third derivative represents the curvature change rate, and a smaller value indicates a smoother function. It can also be used to select segmentation points. This method applies to a wide range of differentiable non-linear functions, such as Sigmoid, Tanh, and Mish (see Appendix IX for details).

Here, we will focus on the piecewise approximation of GeLU. We compute its second derivative, denoted as:

$$F''(x) = \frac{e^{-\frac{x^2}{2}}}{\sqrt{2\pi}} \cdot (2 - x^2) \quad (25)$$

By setting $F''(x) = 0$, we obtain the inflection point $x_1 = \pm\sqrt{2}$. Through the computation of the third derivative $F'''(x)$, we observe that the $F''(x)$ and $F'''(x)$ tend towards zero when $x_2 = \pm 5.075$. Consequently, we choose this point as the second endpoint. With the segmentation points determined

x_1 and x_2 , we can leverage the numpy.polyfit API to find the approximates F_1, F_2 and F_3 . And to ensure the robustness of the approximate GeLU function, we add $\epsilon = 10^{-5}$. The approximate substitution of the Gelu function is as follows:

$$\text{seg5GeLU}(x) = \begin{cases} \epsilon, & \text{if } x < -5.075 \\ F_1(x), & \text{if } -5.075 \leq x < -\sqrt{2} \\ F_2(x), & \text{if } -\sqrt{2} \leq x < \sqrt{2} \\ F_3(x), & \text{if } \sqrt{2} \leq x < 5.075 \\ x + \epsilon, & \text{if } x \geq 5.075 \end{cases} \quad (26)$$

For the interval functions F_1, F_2 and F_3 , we refer the reader to Appendix IX-A

E. Secure GeLU Π_{gelu}

This subsection introduces the secure GeLU Π_{gelu} . Before calculating Π_{gelu} , we first attempt to handle the GeLU function, described in Eq. (7).

To compute seg5GeLU, we initially calculate F_1, F_2 , and F_3 . Given the SIMD ciphertext $\llbracket \mathbf{X} \rrbracket_{\mathcal{A}}$, ϵ , and $\llbracket \mathbf{X} \boxplus \epsilon \rrbracket_{\mathcal{A}}$ are held by \mathcal{B} , we calculate $\llbracket \mathbf{X}^2 \rrbracket_{\mathcal{A}} = \text{BFV.Square}(\llbracket \mathbf{X} \rrbracket_{\mathcal{A}})$, $\llbracket \mathbf{X}^3 \rrbracket_{\mathcal{A}} = \text{BFV.HMult}(\llbracket \mathbf{X}^2 \rrbracket_{\mathcal{A}}, \llbracket \mathbf{X} \rrbracket_{\mathcal{A}})$, $\llbracket \mathbf{X}^4 \rrbracket_{\mathcal{A}} = \text{BFV.Square}(\llbracket \mathbf{X}^2 \rrbracket_{\mathcal{A}})$, subsequently derive $\llbracket F_1 \rrbracket_{\mathcal{A}}$, $\llbracket F_2 \rrbracket_{\mathcal{A}}$, and $\llbracket F_3 \rrbracket_{\mathcal{A}}$ at party \mathcal{B} . Then, we need to select the segment. Hence, we construct $\llbracket \mathbf{X} \rrbracket_{\mathcal{A}} \boxplus \mathbf{R}$, where \mathbf{R} is a uniformly random sampled from \mathbb{Z}_p . Through a round of communication, \mathcal{A} and \mathcal{B} get the secret sharing $\langle \mathbf{X} \rangle_{\mathcal{A}} = \mathbf{X} \ominus \mathbf{R}$, and $\langle \mathbf{X} \rangle_{\mathcal{B}} = \mathbf{R}$, respectively.

These shares must be transformed into the $\mathbb{Z}_{2\kappa}$ from \mathbb{Z}_p . We can directly employ the protocol Π_{LT} in CryptFlow2 [12] for segment selection. \mathcal{A} and \mathcal{B} then locally compute:

$$\begin{aligned} \langle \mathbf{S}_0 \rangle_{\mathcal{P}}^{\mathcal{B}} &= \Pi_{\text{LT}}(\langle \mathbf{X} \rangle_{\mathcal{P}}, -5.075) & \text{if } \langle \mathbf{S}_0 \rangle_{\mathcal{P}}^{\mathcal{B}} = 1, x < -5.075 \\ \langle \mathbf{S}_1 \rangle_{\mathcal{P}}^{\mathcal{B}} &= \Pi_{\text{LT}}(\langle \mathbf{X} \rangle_{\mathcal{P}}, -\sqrt{2}) & \text{if } \langle \mathbf{S}_1 \rangle_{\mathcal{P}}^{\mathcal{B}} = 1, x < -\sqrt{2} \\ \langle \mathbf{S}_2 \rangle_{\mathcal{P}}^{\mathcal{B}} &= \Pi_{\text{LT}}(\sqrt{2}, \langle \mathbf{X} \rangle_{\mathcal{P}}) & \text{if } \langle \mathbf{S}_2 \rangle_{\mathcal{P}}^{\mathcal{B}} = 1, \sqrt{2} < x \\ \langle \mathbf{S}_3 \rangle_{\mathcal{P}}^{\mathcal{B}} &= \Pi_{\text{LT}}(5.075, \langle \mathbf{X} \rangle_{\mathcal{P}}) & \text{if } \langle \mathbf{S}_3 \rangle_{\mathcal{P}}^{\mathcal{B}} = 1, 5.075 < x \end{aligned} \quad (27)$$

Now, we need to compute the sign encoding of the input. We use the XOR (\diamond) operation to obtain sign encoding: b_0, b_1, b_2, b_3, b_4 , s.t.,

$$b_i = 1 \quad \text{iff } x \text{ belongs to the } i\text{-th segment.}$$

\mathcal{A} and \mathcal{B} locally sets :

$$\begin{aligned} \langle \mathbf{b}_0 \rangle_{\mathcal{P}}^{\mathcal{B}} &= \langle \mathbf{S}_0 \rangle_{\mathcal{P}}^{\mathcal{B}} & \text{if } \langle \mathbf{b}_0 \rangle_{\mathcal{P}}^{\mathcal{B}} = 1, x \leq -5.075 \\ \langle \mathbf{b}_1 \rangle_{\mathcal{P}}^{\mathcal{B}} &= \langle \mathbf{S}_0 \rangle_{\mathcal{P}}^{\mathcal{B}} \diamond \langle \mathbf{S}_1 \rangle_{\mathcal{P}}^{\mathcal{B}} & \text{if } \langle \mathbf{b}_1 \rangle_{\mathcal{P}}^{\mathcal{B}} = 1, -5.075 < x \leq -\sqrt{2} \\ \langle \mathbf{b}_2 \rangle_{\mathcal{P}}^{\mathcal{B}} &= \langle \mathbf{S}_1 \rangle_{\mathcal{P}}^{\mathcal{B}} \diamond \langle \mathbf{S}_2 \rangle_{\mathcal{P}}^{\mathcal{B}} & \text{if } \langle \mathbf{b}_2 \rangle_{\mathcal{P}}^{\mathcal{B}} = 1, -\sqrt{2} < x \leq \sqrt{2} \\ \langle \mathbf{b}_3 \rangle_{\mathcal{P}}^{\mathcal{B}} &= \langle \mathbf{S}_2 \rangle_{\mathcal{P}}^{\mathcal{B}} \diamond \langle \mathbf{S}_3 \rangle_{\mathcal{P}}^{\mathcal{B}} & \text{if } \langle \mathbf{b}_3 \rangle_{\mathcal{P}}^{\mathcal{B}} = 1, \sqrt{2} < x \leq 5.075 \\ \langle \mathbf{b}_4 \rangle_{\mathcal{P}}^{\mathcal{B}} &= \langle \mathbf{S}_3 \rangle_{\mathcal{P}}^{\mathcal{B}} & \text{if } \langle \mathbf{b}_4 \rangle_{\mathcal{P}}^{\mathcal{B}} = 1, 5.075 \leq x \end{aligned} \quad (28)$$

Protocol Π_{gelu}

Initialization:

\mathcal{A} and \mathcal{B} generate each private key $sk_{\mathcal{A}}, sk_{\mathcal{B}}$ and public key $pk_{\mathcal{A}}, pk_{\mathcal{B}}$.

inputs:

\mathcal{B} : SIMD-based ciphertext $[[\mathbf{X}]]_{\mathcal{A}}$

Process:

\mathcal{B} : Computes $[[\mathbf{X}]]_{\mathcal{A}}, [[\mathbf{X}^2]]_{\mathcal{A}}, [[\mathbf{X}^3]]_{\mathcal{A}}, [[\mathbf{X}^4]]_{\mathcal{A}}, [[\mathbf{F}_1]]_{\mathcal{A}},$

$[[\mathbf{F}_2]]_{\mathcal{A}}, [[\mathbf{F}_3]]_{\mathcal{A}}$; Generates a uniformly random

$\mathbf{R} \in \mathbb{Z}_p^{d_m \times d_c}$; Flattens \mathbf{R} row-wise to get $\tilde{\mathbf{R}}$; Computes

$[[\mathbf{X}]]_{\mathcal{A}} \boxplus \tilde{\mathbf{R}}$; Denotes $\langle \mathbf{X} \rangle_{\mathcal{A}} = \tilde{\mathbf{R}}$;

\mathcal{A} : Receives $[[\mathbf{X}]]_{\mathcal{A}} \boxplus \tilde{\mathbf{R}}$; Decrypts $[[\mathbf{X}]]_{\mathcal{A}} \boxplus \tilde{\mathbf{R}}$ to obtain $\langle \mathbf{X} \rangle_{\mathcal{B}} = \mathbf{X} \ominus \tilde{\mathbf{R}}$;

\mathcal{P} ^a: Participants \mathcal{A} and \mathcal{B} do the same as follow:

$\langle \mathbf{S}_0 \rangle_{\mathcal{P}}^{\mathcal{B}} =$

$\Pi_{\text{LT}}(\langle \mathbf{X} \rangle_{\mathcal{P}}, -5.075)$ if $\langle \mathbf{S}_0 \rangle_{\mathcal{P}}^{\mathcal{B}} = 1, x < -5.075$

$\langle \mathbf{S}_1 \rangle_{\mathcal{P}}^{\mathcal{B}} = \Pi_{\text{LT}}(\langle \mathbf{X} \rangle_{\mathcal{P}}, -\sqrt{2})$ if $\langle \mathbf{S}_1 \rangle_{\mathcal{P}}^{\mathcal{B}} = 1, x < -\sqrt{2}$

$\langle \mathbf{S}_2 \rangle_{\mathcal{P}}^{\mathcal{B}} = \Pi_{\text{LT}}(\sqrt{2}, \langle \mathbf{X} \rangle_{\mathcal{P}})$ if $\langle \mathbf{S}_2 \rangle_{\mathcal{P}}^{\mathcal{B}} = 1, \sqrt{2} < x$

$\langle \mathbf{S}_3 \rangle_{\mathcal{P}}^{\mathcal{B}} = \Pi_{\text{LT}}(5.075, \langle \mathbf{X} \rangle_{\mathcal{P}})$ if $\langle \mathbf{S}_3 \rangle_{\mathcal{P}}^{\mathcal{B}} = 1, 5.075 < x$

Then \mathcal{P} locally sets:

$\langle \mathbf{b}_0 \rangle_{\mathcal{P}}^{\mathcal{B}} = \langle \mathbf{S}_0 \rangle_{\mathcal{P}}^{\mathcal{B}}$ if $\langle \mathbf{b}_0 \rangle_{\mathcal{P}} = 1, x \leq -5.075$

$\langle \mathbf{b}_1 \rangle_{\mathcal{P}}^{\mathcal{B}} =$

$\langle \mathbf{S}_0 \rangle_{\mathcal{P}}^{\mathcal{B}} \diamond \langle \mathbf{S}_1 \rangle_{\mathcal{P}}^{\mathcal{B}}$ if $\langle \mathbf{b}_1 \rangle_{\mathcal{P}}^{\mathcal{B}} = 1, -5.075 < x \leq -\sqrt{2}$

$\langle \mathbf{b}_2 \rangle_{\mathcal{P}}^{\mathcal{B}} = \langle \mathbf{S}_1 \rangle_{\mathcal{P}}^{\mathcal{B}} \diamond \langle \mathbf{S}_2 \rangle_{\mathcal{P}}^{\mathcal{B}}$ if $\langle \mathbf{b}_2 \rangle_{\mathcal{P}}^{\mathcal{B}} = 1, -\sqrt{2} < x \leq \sqrt{2}$

$\langle \mathbf{b}_3 \rangle_{\mathcal{P}}^{\mathcal{B}} = \langle \mathbf{S}_2 \rangle_{\mathcal{P}}^{\mathcal{B}} \diamond \langle \mathbf{S}_3 \rangle_{\mathcal{P}}^{\mathcal{B}}$ if $\langle \mathbf{b}_3 \rangle_{\mathcal{P}}^{\mathcal{B}} = 1, \sqrt{2} < x \leq 5.075$

$\langle \mathbf{b}_4 \rangle_{\mathcal{P}}^{\mathcal{B}} = \langle \mathbf{S}_3 \rangle_{\mathcal{P}}^{\mathcal{B}}$ if $\langle \mathbf{b}_4 \rangle_{\mathcal{P}}^{\mathcal{B}} = 1, 5.075 \leq x$

\mathcal{P} converts the bool secret sharing to additive sharing,

gets $\mathbf{b}_i + 2^f \equiv \langle \mathbf{b}_i \rangle_{\mathcal{A}} + \langle \mathbf{b}_i \rangle_{\mathcal{B}} \pmod{2^k}$.

\mathcal{A} : Computes $\langle \mathbf{b}_i \rangle_{\mathcal{A}} \ominus 2^f$; Encrypts $\langle \mathbf{b}_i \rangle_{\mathcal{A}} \ominus 2^f$ to get

$[[\langle \mathbf{b}_i \rangle_{\mathcal{A}} \ominus 2^f]]_{\mathcal{A}}$; Sends $[[\langle \mathbf{b}_i \rangle_{\mathcal{A}} \ominus 2^f]]_{\mathcal{A}}$ to \mathcal{B} .

\mathcal{B} : Receives $[[\langle \mathbf{b}_i \rangle_{\mathcal{A}} \ominus 2^f]]_{\mathcal{A}}$; Computes $[[\mathbf{b}_i]]_{\mathcal{A}} = \langle \mathbf{b}_i \rangle_{\mathcal{B}}$

$\boxplus [[\langle \mathbf{b}_i \rangle_{\mathcal{A}} \ominus 2^f]]_{\mathcal{A}}$ to get $[[\mathbf{b}]]_{\mathcal{A}} = [[\mathbf{b}_0, \mathbf{b}_1, \mathbf{b}_2, \mathbf{b}_3, \mathbf{b}_4]]_{\mathcal{A}}$;

Computes $[[\mathbf{Y}]]_{\mathcal{A}} = [[\mathbf{b}_0]]_{\mathcal{A}} \boxplus \epsilon \boxplus [[\mathbf{b}_1]]_{\mathcal{A}} \boxplus [[\mathbf{F}_1]]_{\mathcal{A}} \boxplus$

$[[\mathbf{b}_2]]_{\mathcal{A}} \boxplus [[\mathbf{F}_2]]_{\mathcal{A}} \boxplus [[\mathbf{b}_3]]_{\mathcal{A}} \boxplus [[\mathbf{F}_3]]_{\mathcal{A}} \boxplus [[\mathbf{b}_4]]_{\mathcal{A}} \boxplus [[\mathbf{F}_4]]_{\mathcal{A}}$;

Generates uniformly random $\mathbf{N} \in \mathbb{Z}_p^{d_m \times d_c}$; Computes

$[[\langle \mathbf{Y} \rangle_{\mathcal{A}}]]_{\mathcal{A}} = [[\mathbf{Y}]]_{\mathcal{A}} \boxplus \mathbf{N}$; Sends $[[\langle \mathbf{Y} \rangle_{\mathcal{A}}]]_{\mathcal{A}}$ to \mathcal{A} .

\mathcal{A} : Receives $[[\langle \mathbf{Y} \rangle_{\mathcal{A}}]]_{\mathcal{A}} \boxplus \mathbf{N}$.

Private outputs:

\mathcal{A} : $\langle \mathbf{Y} \rangle_{\mathcal{A}} = \text{BFV.Decrypt}(sk_{\mathcal{A}}, [[\langle \mathbf{Y} \rangle_{\mathcal{A}}]]_{\mathcal{A}} \boxplus \mathbf{N})$

\mathcal{B} : $\langle \mathbf{Y} \rangle_{\mathcal{B}} = \mathbf{N}$

^aSince \mathcal{A} and \mathcal{B} follow the same computation steps, we denote them as $\mathcal{P} \in \{\mathcal{A}, \mathcal{B}\}$. Before execution, $\langle \mathbf{X} \rangle_{\mathcal{A}}$ and $\langle \mathbf{X} \rangle_{\mathcal{B}}$ are transformed from the \mathbb{Z}_p to the \mathbb{Z}_{2^k} .

Fig. 6: Secure GeLU Π_{gelu}

Subsequently, the bool secret sharing is converted to additive secret sharing by using Π_{B2A} ⁵. Since we employ a fixed-point representation where an input number x is defined as $\lfloor \bar{x} \cdot 2^s \rfloor \pmod{2^k}$, the additive secret sharing yields a result of $\mathbf{b}_i + 2^s \equiv \langle \mathbf{b}_i \rangle_{\mathcal{A}} + \langle \mathbf{b}_i \rangle_{\mathcal{B}} \pmod{p}$, $\mathbf{b}_i \in \{0, 1\}$. encrypting $\langle \mathbf{b}_i \rangle_{\mathcal{A}}$, party \mathcal{A} sends $[[\langle \mathbf{b}_i \rangle_{\mathcal{A}}]]_{\mathcal{A}}$ to \mathcal{B} . \mathcal{B} computes:

$$[[\mathbf{b}_i]]_{\mathcal{A}} = \langle \mathbf{b}_i \rangle_{\mathcal{B}} \boxplus [[\langle \mathbf{b}_i \rangle_{\mathcal{A}}]]_{\mathcal{A}} \boxplus 2^s \quad (29)$$

Finally, the GeLU function can be represented as:

$$\text{GeLU}(x) = b_0 \epsilon + b_1 F_1(x) + b_2 F_2(x) + b_3 F_3(x) + b_4(x + \epsilon) \quad (30)$$

⁵The protocol Π_{B2A} can convert the bool secret sharing to additive secret sharing, which is also from Cryptflow2 [12]

In conclusion, \mathcal{B} obtains the ciphertext result of GeLU, and the specific procedure is shown in Fig 6.

IV. EVALUATION

A. Experimental Setup

Implementation: FASTLMPI is implemented in C++ and we use EMP toolkit⁶ [27] to implement communication between the parties. Leveraging the SCI⁷ library in EzPC [28] for fixed-point numerical computations and SEAL⁸ [26] library for BFV homomorphic encryption. FASTLMPI and extern libraries are compiled by GCC (version 11.4.0) on Ubuntu 22.04.

Testbed Environment: All the following experiments were performed on a rack server with the Intel(R) Xeon(R) Gold 6238R CPU @ 2.20GHz and 377 gigabytes of RAM. We control the communication bandwidth using the Linux Traffic Control (tc) command. We simulate two different WAN environments, which are $\text{WAN}_1 = \{400\text{Mbps}, 10 \text{ ms}\}$ and $\text{WAN}_2 = \{200\text{Mbps}, 40 \text{ ms}\}$.

Concrete SEAL's and SS's Parameters: This paper uses bit-length $k = 37$ and precision $s = 12$ for the expressed of fixed-point numbers, and using the SEAL parameters $\text{HE}_{\text{SCI}} = \{N = 8192, q \approx 180, p \approx 29\}$ (Similar to [6], [29]) for HE.

Model Architectures: We measure the performance of FASTLMPI on BERT_{BASE} [30] and denote the number of layers (i.e., Transformer blocks) as L , the hidden size as H , and the number of the self-attention head as A . The size of feed-forward is $4H$, i.e., 3072 for the $H = 768$ and $L = 12$.

Metrics: We test on four datasets from the GLUE [31] benchmark, which is widely used to evaluate the model performance. We use four datasets in GLUE, consisting of three classification tasks: MRPC, RTE, and SST-2.

B. Microbenchmarks

1) *Secure matrix multiplication:* We first compare the performance of secure matrix multiplication with SCI_{OT} [12] and FIT_{FC} [13] under three network environments: LAN, WAN_1 , and WAN_2 . The results are shown in Tab. II. Our method outperforms the baseline methods in terms of communication and running time in most scenarios. Particularly, in the LAN network environment with a matrix dimension of $128 \times 256 \times 64$, our method achieves a $15.3 \times$ and $6.0 \times$ speedup compared to FIT_{FC} and SCI_{OT} , respectively.

We also benchmarked the performance of linear_1 ⁹ against SOTA methods IRON [33] and BOLT [6]. The results are presented in Tab. III

The key takeaway is that our run time is 0.32 seconds, and the communication cost is 271.47 MB. In contrast to FIT_{FC} and BOLT that leverage HE, our approach offers a 15.9-fold and 39.7-fold improvement in runtime under LAN

⁶<https://github.com/emp-toolkit/emp-tool>

⁷<https://github.com/mpc-msri/EzPC/tree/master/SCI>

⁸<https://github.com/microsoft/SEAL>

⁹ linear_1 is the matrix multiplication operation in the first layer of BERT_{base}: $\mathbf{X}^{128 \times 768} \otimes \mathbf{W}^{768 \times 64}$

TABLE II: Performance comparison of secure matrix multiplication. Timing results are averaged from 5 runs

Method	Time (ms) under LAN		
	FIT _{FC} [32]	SCI _{OT} [12]	Π_{matmul}
32 × 32 × 64	1296	84	37
128 × 64 × 64	1370	288	41
128 × 256 × 64	2462	962	161
256 × 256 × 64	2492	1729	210
Time (ms) under WAN ₁			
32 × 32 × 64	2470	533	335
128 × 64 × 64	2964	1151	489
128 × 256 × 64	4670	4576	2014
256 × 256 × 64	4421	10931	4123
Time (ms) under WAN ₂			
32 × 32 × 64	4796	2032	1075
128 × 64 × 64	5236	4045	1301
128 × 256 × 64	7772	12733	4647
256 × 256 × 64	7919	17203	9913
Comm. (MB)			
32 × 32 × 64	62.13	4.12	11.65
128 × 64 × 64	67.78	29.12	22.95
128 × 256 × 64	101.67	123.93	90.72
256 × 256 × 64	101.67	241.95	181.44

TABLE III: Comparison of linear₁ with SOTA in terms of running time and communication costs. Timing results are averaged from 5 runs

Method		Time (s)			Comm.(MB)
		LAN	WAN ₁	WAN ₂	
Linear ₁	FIT _{FC} [32]	5.09	8.51	13.92	192.04
	SCI _{OT} [12]	2.56	9.92	25.68	406.16
	IRON [33]	6.86	8.35	33.44	4844.14
	BOLT [6]	12.70	13.02	13.78	7.06
	Π_{matmul}	0.32	6.09	12.62	271.47

setting, respectively. Furthermore, in comparison with SS-based SCI_{OT}, our communication costs are reduced by 1.5×. Our approach offers substantial improvements in terms of runtime and communication cost, particularly in LAN settings. Given the other three linear layers in FeedForward, we leverage the BSGS algorithm from BOLT to execute matrix multiplication directly on encrypted data.

2) *Secure Non-linear*: We conducted a comprehensive evaluation of the non-linear functions (SoftMax, LayerNorm, and GeLU¹⁰) embedded in Bert_{base} under three network environments (LAN, WAN₁, WAN₂), addressing the long-standing challenge of nonlinearity in TBM private inference. Results are presented in Tab. IV.

Our findings reveal that the non-linear protocol within FASTLMPI offers substantial performance gains across various network environments. Specifically, Π_{softmax} surpasses IRON

¹⁰The GeLU in BOLT is the version without preprocessing

TABLE IV: Comparison of non-linear computation with SOTA in terms of running time and communication costs. Timing results are averaged from 5 runs

Method		Time (s)			Comm.(MB)
		LAN	WAN ₁	WAN ₂	
SoftMax	IRON [33]	5.36	23.25	129.82	3356.92
	BOLT [6]	1.96	15.92	76.67	1285.13
	FASTLMPI	0.14	0.31	0.99	4.94
LayerNorm	IRON [33]	10.02	23.25	57.11	786.38
	BOLT [6]	1.82	15.92	51.31	844.6
	FASTLMPI	0.92	4.25	23.23	154.69
GeLU	IRON [33]	10.30	106.31	246.39	7524
	BOLT [6]	4.33	36.18	101.84	2769.89
	FASTLMPI	1.99	14.50	45.39	928.77

by achieving a 38.3×, 75×, and 131.13× speedup in runtime under LAN, WAN₁, WAN₂, respectively, while reducing communication costs by 679.5×. Compared to the state-of-the-art BOLT, Π_{softmax} demonstrates even more impressive results, with a 14×, 51.4×, and 77.4× speedup and a 260.2-fold reduction in communication costs.

3) *Accuracy evaluation of seg5GeLU*: Fig. 7 presents the visualization results and accuracy evaluation of seg5Gelu within a specific range. Specifically, we evaluated the Mean Absolute Error (MAE) of various segmentation methods using a dataset of 10,000 points spanning the range of -6 to 6. The conclusion is that our proposed method achieves a 4.5-fold and 1.3-fold MAE reduction compared to Bumblebee and BOLT, respectively. More notably, by carefully selecting specific points for piecewise polynomial fitting of GeLU, we achieve accuracy comparable to BubbleBee [7], PUMA [10] (with 6-degree polynomials), and SecFormer [34] (with 7-degree polynomials) using only 3-degree polynomials. Consequently, our approach naturally surpasses BOLT when using 4-degree polynomials.

To further underscore the extensibility of our method, We also fitted Sigmoid, Tanh, and Mish functions, and the results show that our method achieves a lower MAE and polynomial degree As depicted in Fig. 8a and Fig. 8b, our fitting results exhibit significantly higher accuracy compared to [35]–[38]. Furthermore, as shown in Fig. 8c and Fig. 8d, the superiority of our method is consistent across different partition points. These findings strongly support the effectiveness of selecting specific points for function fitting. We also evaluated the applicability of our proposed method to the Tanh and Mish activation functions.

Similar to Sigmoid’s testing method, we evaluate the MAE of Tanh fitted at different points in the set {0.5, 2, 3, 4} and at the partition points selected by our method. As shown in Fig. 9, the results demonstrate the effectiveness of our approach.

As Tanh, BOLT uses a 5-degree polynomial to approximate it, we achieve higher accuracy with only a 4-degree polynomial. The evaluation of Mish in Fig. 10 provides additional validation that our approach of selecting specific points for piecewise fitting can improve accuracy.

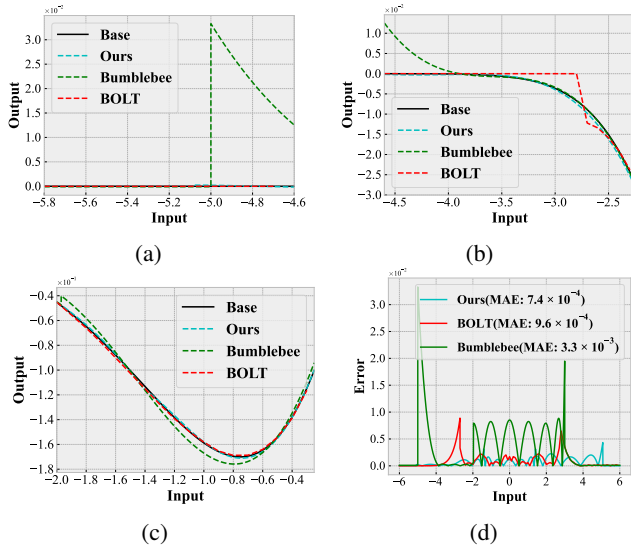


Fig. 7: Comparative analysis of GeLU function

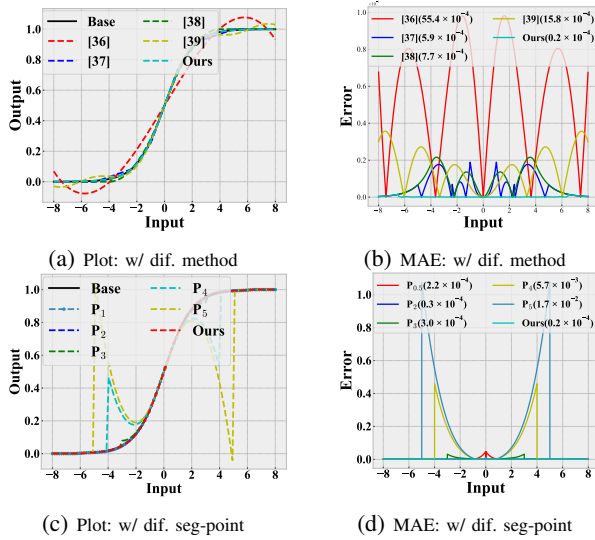


Fig. 8: Comparative analysis of Sigmoid

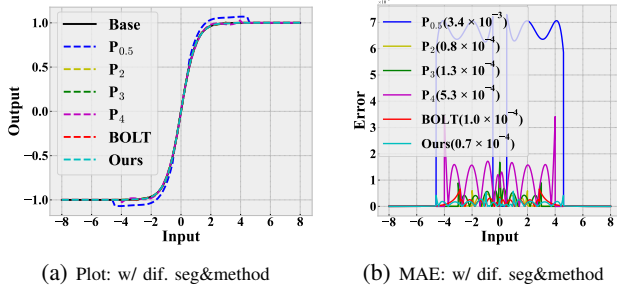


Fig. 9: Comparative analysis of Tanh

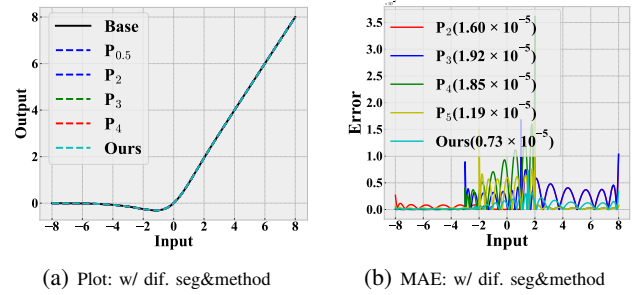


Fig. 10: Comparative analysis of Mish

C. Evaluation on BERT_{base}

1) *Accuracy*: In Tab V, we evaluated the F1 score on MRPC, RTE, and SST-2 accuracy. We followed the data setting in BOLT¹¹. We only modified the GeLU activation function for a fair comparison while keeping other components unchanged. Our method does not require re-training the model as in MPCformer, nor fine-tuning as in BOLT. Baseline uses GeLU as described in Eq. (7), and is otherwise identical to BOLT.

TABLE V: Accuracy of floating-point plaintext, Baseline, BOLT, and FASTLMPI

Dataset	Metric	[39] (STD)	BERT baseline	BOLT [6] w/o W.E.	FASTLMPI
MRPC	F1	90 (0.23)	89.8	86.7	89.1
RTE	Accuracy	69.7 (1.5)	54.5	65.0	54.5
SST-2	Accuracy	92.4 (0.59)	89.5	90.5	90.7

RET-BOLT-Acc.: =65.0, which may be due to the model parameters re-training by BOLT.

2) *End-to-End inference*: In Tab. VI, we compare the performance of FASTLMPI with other private TBM inference methods. Similar to NEXUS [9], the end-to-end performance is the aggregation of the microbenchmarks. In summary, we have achieved a 2.8-fold, 2.2-fold, and 2.6-fold improvement in inference time under three network settings and a reduction of communication costs by 72.2% compared to the BOLT.

TABLE VI: End-to-end comparisons with existing private inference frameworks. The numbers of SIGMA, NEXUS, and BumbleBee are taken from their papers. Frameworks marked with "*" are not 2PC framework.

Method	Time (s)			Comm.(GB)
	LAN	WAN ₁	WAN ₂	
NEXUS [9]	≈ 857	≈ 869	≈ 881	0.16
IRON [33]	417.08	4037.97	9525.28	272.22
BOLT [6] w/o W.E.	369.19	1502.12	3784.39	72.21
SIGMA* [40]	≈ 240.0	-	-	34.37
BumbleBee [7]	≈ 204.0	≈ 971.0	≈ 1578.0	8.58
FASTLMPI	131.36	679.90	1479.82	20.49

¹¹Model wights are available here: <https://drive.google.com/drive/u/0/folders/13bBok39UevQ-6hDWHtBVtLJrYVo5VnsR>,

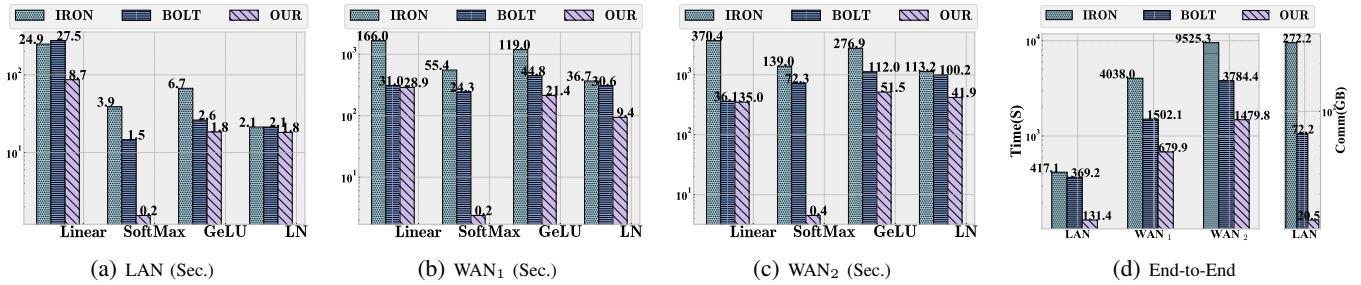


Fig. 11: End-to-End linear & non-linear operators' performance.

It is noteworthy that NEXUS exhibits a more significant advantage in scenarios with higher network latency. This is because NEXUS is a non-interactive approach that employs a unified HE technique. However, when network latency is low, FASTLMPI still holds a substantial advantage. We also evaluated the performance of IRON, BOLT, and FASTLMPI under LAN, WAN₁, and WAN₂ network conditions in the end-to-end inference task. Fig. 11 shows linear and non-linear operators' inference time and communication costs. Π_{softmax} benefits the most from the fine-grained collaborative technology of HE and SS, experiencing a 9 – 72 \times speedup in runtime and a 260 – 769 \times reduction in communication cost.

V. RELATED WORK

With the proliferation of Deep Learning, private inference has become a key area of research.

Private inference with efficient protocols: Many methods for privacy protection in large models are implemented through the design of efficient protocols, such as [7], [9], [24], [34], [41], [42], [43]. Where [7] has optimized the matrix multiplication protocol via a specialized RLWE batching technique, provided methods for designing efficient and accurate protocols for the activation functions used in transformers, and has successfully run BumbleBee on five pre-trained transformer models. And NEXUS [9] designs a non-interactive private transformer inference using HE, achieving efficient inference under the WAN environment. They provide SIMD-based ciphertext slot folding and decompression techniques to reduce communication costs. Tan et al. [44] introduce CryptGPU, which identifies a sequence of “GPU-friendly” cryptographic protocols to enable privacy-preserving evaluation of both linear and non-linear operations on the GPU.

Private inference with hardware acceleration: Due to the high computational resource consumption of some cryptographic primitives, some works adopt hardware acceleration methods to improve the efficiency of private computations, as in [40], [45], [46], [47], [48]. Among them, SIGMA [40] enhances inference efficiency through GPU while maintaining model accuracy based on Function secret sharing (FSS) [49]. It is worth noting that SIGMA is the first work to design a 2-PC private TBM inference by using the FSS technique and accelerating it with GPU. RRNet [45] replaces computationally

expensive ReLU operations with trainable polynomial activation functions, develops a cryptographic hardware scheduler and performance model for FPGA platforms, constructs a latency lookup table to optimize the scheduling of encrypted operations.

Private inference with quantization and distillation: Some studies also employ quantization and distillation methods to reduce the model size, thereby enhancing the efficiency of privacy-preserving computations. SecFormer [34] and MPCFormer [50] utilize knowledge distillation to train a surrogate Transformer model with fewer parameters and simpler architecture, achieving performance comparable to the original Transformer. The surrogate model is both high-performing and compatible with SMPC. MPCViT [51], based on the vision transformer, replaces the Softmax with an accurate and MPC-friendly ReLU Softmax. An MPC-aware differentiable NAS [52] algorithm that can learn architectural parameters and model parameters simultaneously and finally uses knowledge distillation to improve the accuracy.refe

VI. DISCUSSION

Extensibility of FASTLMPI: A specific benchmark is provided on the BERT_{base} model. FASTLMPI, enabled by the four fundamental protocols we provide, can be applied to transformer-based language models including GPT [53], BERT_{large}, and so on. Moreover, the offered activation functions (Sigmoid, Tanh, and Mish) are well-suited for traditional neural networks like Logistic regression [54], LSTM [55], and RNN [56].

The gains from fine-grained co-design of HE and SS: It is well known that, classical arts use HE in linear computations (Matmul), and SS in non-linear computations (Softmax, Layer-Norm, GeLU). However, in some special cases, preprocessing ciphertexts in SIMD form before homomorphic operations can bring greater benefits than SS. This is our original intention: to selectively use HE in Softmax, LayerNorm, and GeLU while selectively using SS in Matmul, breaking the boundaries of operators of using HE solely in matrix multiplication and SS solely in non-linear operations, aiming to reduce computational and communication costs simultaneously. Our experiments have verified that this is feasible. rrin

VII. CONSLUSION & FUTURE WORK

We introduce FASTLMPI, an optimized 2PC private TBM inference framework, which significantly reduces costs compared to previous methods. This advancement enhances the practicality of secure inference for the TBM. Moreover, we draw two key conclusions. Firstly, through the strategic collaboration of Homomorphic Encryption (HE) and secret sharing (SS), all homomorphic operations are transformed into ciphertext-plaintext multiplications. This allows exploration of Partial Homomorphic Encryption algorithms like Paillier [57], [58] and ECC-Elgamal [59], [60], [61] for more efficient HE&SS-based protocols. Secondly, breaking the linear and nonlinear boundaries significantly improves performance, with a higher emphasis on HE making private TBM inference more suitable for WAN environments with poor network conditions, while a heavier reliance on SS provides an advantage in LAN environments.

In future work, creating a network environment-adaptive private TBM inference framework using feedback tuning mechanisms is a key objective, which can dynamically generate the optimal private TBM inference scheme tailored to the prevailing network conditions. The secure computing protocol used in the generation scheme can directly call the existing mature private computing library. But it is also possible to redesign the base protocol to be more efficient. So we believe that the feedback mechanism of the cost model and designing efficient protocols do not conflict and are equally important for driving the development of Privacy-preserving Machine Learning.

REFERENCES

- [1] C. Dong, J. Weng, J. Liu, Y. Zhang, Y. Tong, A. Yang, Y. Cheng, and S. Hu, "Fusion: Efficient and secure inference resilient to malicious servers," 2023.
- [2] N. Singh and A. K. Singh, "Data privacy protection mechanisms in cloud," *Data Science and Engineering*, vol. 3, no. 1, pp. 24–39, 2018.
- [3] G. Su, J. Wang, X. Xu, Y. Wang, and C. Wang, "The utilization of homomorphic encryption technology grounded on artificial intelligence for privacy preservation," *International Journal of Computer Science and Information Technology*, vol. 2, no. 1, pp. 52–58, 2024.
- [4] S. E. V. S. Pillai and K. Polimetla, "Enhancing network privacy through secure multi-party computation in cloud environments," pp. 1–6, 2024.
- [5] A. Vaswani, N. Shazeer, N. Parmar, J. Uszkoreit, L. Jones, A. N. Gomez, L. Kaiser, and I. Polosukhin, "Attention is all you need," *Advances in neural information processing systems*, vol. 30, 2017.
- [6] Q. Pang, J. Zhu, H. Mollering, Z. Wenting, and T. Schneider, "Bolt: Privacy-preserving, accurate and efficient inference for transformers," 2024.
- [7] W.-j. Lu, Z. Huang, Z. Gu, J. Li, J. Liu, K. Ren, C. Hong, T. Wei, and W. Chen, "Bumblebee: Secure two-party inference framework for large transformers," *Cryptology ePrint Archive*, 2023.
- [8] H. Ghodosi, J. Pieprzyk, and R. Steinfeld, "Multi-party computation with conversion of secret sharing," *Designs, Codes and Cryptography*, vol. 62, pp. 259–272, 2012.
- [9] J. Zhang, J. Liu, X. Yang, Y. Wang, K. Chen, X. Hou, K. Ren, and X. Yang, "Secure transformer inference made non-interactive," *Cryptology ePrint Archive*, 2024.
- [10] Y. Dong, W.-j. Lu, Y. Zheng, H. Wu, D. Zhao, J. Tan, Z. Huang, C. Hong, T. Wei, and W. Cheng, "Puma: Secure inference of llama-7b in five minutes," *arXiv preprint arXiv:2307.12533*, 2023.
- [11] K. Cong, D. Das, J. Park, and H. V. Pereira, "Sortinghat: Efficient private decision tree evaluation via homomorphic encryption and transcribing," in *Proceedings of the 2022 ACM SIGSAC Conference on Computer and Communications Security*, 2022, pp. 563–577.
- [12] D. Rathee, M. Rathee, N. Kumar, N. Chandran, D. Gupta, A. Rastogi, and R. Sharma, "Cryptflow2: Practical 2-party secure inference," in *Proceedings of the 2020 ACM SIGSAC Conference on Computer and Communications Security*, 2020, pp. 325–342.
- [13] Q. Zhang, T. Xiang, C. Xin, and H. Wu, "United we stand: Accelerating privacy-preserving neural inference by conjunctive optimization with interleaved nexus," vol. 38, no. 15, pp. 16794–16802, 2024.
- [14] Y. Lindell, "How to simulate it—a tutorial on the simulation proof technique," *Tutorials on the Foundations of Cryptography: Dedicated to Oded Goldreich*, pp. 277–346, 2017.
- [15] R. L. Rivest, L. Adleman, M. L. Dertouzos *et al.*, "On data banks and privacy homomorphisms," *Foundations of secure computation*, vol. 4, no. 11, pp. 169–180, 1978.
- [16] Z. Brakerski, "Fully homomorphic encryption without modulus switching from classical gapsvp," pp. 868–886, 2012.
- [17] I. Chillotti, N. Gama, M. Georgieva, and M. Izabachene, "Faster fully homomorphic encryption: Bootstrapping in less than 0.1 seconds," pp. 3–33, 2016.
- [18] V. Lyubashevsky, C. Peikert, and O. Regev, "On ideal lattices and learning with errors over rings," pp. 1–23, 2010.
- [19] J. Fan and F. Vercauteren, "Somewhat practical fully homomorphic encryption," *Cryptology ePrint Archive*, 2012.
- [20] N. P. Smart and F. Vercauteren, "Fully homomorphic simd operations," *Designs, codes and cryptography*, vol. 71, pp. 57–81, 2014.
- [21] P. Mohassel and P. Rindal, "Aby3: A mixed protocol framework for machine learning," pp. 35–52, 2018.
- [22] Y. Akimoto, K. Fukuchi, Y. Akimoto, and J. Sakuma, "Privformer: Privacy-preserving transformer with mpc," in *2023 IEEE 8th European Symposium on Security and Privacy (EuroS&P)*. IEEE, 2023, pp. 392–410.
- [23] X. Liu, Z. Liu, Q. Li, K. Xu, and M. Xu, "Pencil: Private and extensible collaborative learning without the non-colluding assumption," *arXiv preprint arXiv:2403.11166*, 2024.
- [24] F. Liu, X. Xie, and Y. Yu, "Scalable multi-party computation protocols for machine learning in the honest-majority setting," in *33rd USENIX Security Symposium (USENIX Security 23)*, 2024.
- [25] D. Rathee, M. Rathee, R. K. K. Goli, D. Gupta, R. Sharma, N. Chandran, and A. Rastogi, "Sirnn: A math library for secure rnn inference," in *2021 IEEE Symposium on Security and Privacy (SP)*. IEEE, 2021, pp. 1003–1020.
- [26] "Microsoft SEAL (release 4.1)," <https://github.com/Microsoft/SEAL>, Jan. 2023, microsoft Research, Redmond, WA.
- [27] X. Wang, A. J. Malozemoff, and J. Katz, "EMP-toolkit: Efficient Multi-Party computation toolkit," <https://github.com/emp-toolkit>, 2016.
- [28] N. Chandran, D. Gupta, A. Rastogi, R. Sharma, and S. Tripathi, "Ezpc: Programmable and efficient secure two-party computation for machine learning," in *2019 IEEE European Symposium on Security and Privacy (EuroS&P)*. IEEE, 2019, pp. 496–511.
- [29] Z. Huang, W. j. Lu, C. Hong, and J. Ding, "Cheetah: Lean and fast secure {Two-Party} deep neural network inference," in *31st USENIX Security Symposium (USENIX Security 22)*, 2022, pp. 809–826.
- [30] J. Devlin, M.-W. Chang, K. Lee, and K. Toutanova, "Bert: Pre-training of deep bidirectional transformers for language understanding," *arXiv preprint arXiv:1810.04805*, 2018.
- [31] A. Wang, A. Singh, J. Michael, F. Hill, O. Levy, and S. R. Bowman, "Glue: A multi-task benchmark and analysis platform for natural language understanding," *arXiv preprint arXiv:1804.07461*, 2018.
- [32] Q. Zhang, T. Xiang, C. Xin, and H. Wu, "From individual computation to allied optimization: Remodeling privacy-preserving neural inference with function input tuning," 2024.
- [33] M. Hao, H. Li, H. Chen, P. Xing, G. Xu, and T. Zhang, "Iron: private inference on transformers," *Proceedings of the 36th International Conference on Neural Information Processing Systems (NIPS '22)*, p. 15718–15731, 2022.
- [34] J. Luo, Y. Zhang, J. Zhang, X. Mu, H. Wang, Y. Yu, and Z. Xu, "Secformer: Towards fast and accurate privacy-preserving inference for large language models," *arXiv preprint arXiv:2401.00793*, 2024.

- [35] J. Chiang, "Privacy-preserving logistic regression training on large datasets," *arXiv preprint arXiv:2406.13221*, 2024.
- [36] H. Amin, K. M. Curtis, and B. R. Hayes-Gill, "Piecewise linear approximation applied to nonlinear function of a neural network," *IEEE Proceedings-Circuits, Devices and Systems*, vol. 144, no. 6, pp. 313–317, 1997.
- [37] S. Ngah and R. A. Bakar, "Sigmoid function implementation using the unequal segmentation of differential lookup table and second order nonlinear function," *Journal of Telecommunication, Electronic and Computer Engineering (JTEC)*, vol. 9, no. 2-8, pp. 103–108, 2017.
- [38] Y. Zheng, Q. Zhang, S. S. Chow, Y. Peng, S. Tan, L. Li, and S. Yin, "Secure softmax/sigmoid for machine-learning computation," in *Proceedings of the 39th Annual Computer Security Applications Conference*, 2023, pp. 463–476.
- [39] O. Zafir, G. Boudoukh, P. Izsak, and M. Wasserblat, "Q8bert: Quantized 8bit bert," pp. 36–39, 2019.
- [40] K. Gupta, N. Jawalkar, A. Mukherjee, N. Chandran, D. Gupta, A. Panwar, and R. Sharma, "Sigma: Secure gpt inference with function secret sharing," *Cryptology ePrint Archive*, 2023.
- [41] S. Kundu, S. Lu, Y. Zhang, J. Liu, and P. A. Beereel, "Learning to linearize deep neural networks for secure and efficient private inference," *arXiv preprint arXiv:2301.09254*, 2023.
- [42] T. Chen, H. Bao, S. Huang, L. Dong, B. Jiao, D. Jiang, H. Zhou, J. Li, and F. Wei, "THE-X: Privacy-preserving transformer inference with homomorphic encryption," in *Findings of the Association for Computational Linguistics: ACL 2022*, S. Muresan, P. Nakov, and A. Villavicencio, Eds. Dublin, Ireland: Association for Computational Linguistics, May 2022, pp. 3510–3520.
- [43] X. Hou, J. Liu, J. Li, Y. Li, W.-j. Lu, C. Hong, and K. Ren, "Ciphertgt: Secure two-party gpt inference," *Cryptology ePrint Archive*, 2023.
- [44] S. Tan, B. Knott, Y. Tian, and D. J. Wu, "Cryptgpu: Fast privacy-preserving machine learning on the gpu," in *2021 IEEE Symposium on Security and Privacy (SP)*. IEEE, 2021, pp. 1021–1038.
- [45] H. Peng, S. Zhou, Y. Luo, N. Xu, S. Duan, R. Ran, J. Zhao, S. Huang, X. Xie, C. Wang *et al.*, "Rmet: Towards relu-reduced neural network for two-party computation based private inference," *arXiv preprint arXiv:2302.02292*, 2023.
- [46] J.-L. Watson, S. Wagh, and R. A. Popa, "Piranha: A {GPU} platform for secure computation," in *31st USENIX Security Symposium (USENIX Security 22)*, 2022, pp. 827–844.
- [47] N. Jawalkar, K. Gupta, A. Basu, N. Chandran, D. Gupta, and R. Sharma, "Orca: Fss-based secure training and inference with gpus," *Cryptology ePrint Archive*, 2023.
- [48] H. Yang, S. Shen, S. Jiang, L. Zhou, W. Dai, and Y. Zhao, "Xnet: A real-time unified secure inference framework using homomorphic encryption," *Cryptology ePrint Archive*, 2023.
- [49] E. Boyle, N. Gilboa, and Y. Ishai, "Function secret sharing: Improvements and extensions," in *Proceedings of the 2016 ACM SIGSAC Conference on Computer and Communications Security*, 2016, pp. 1292–1303.
- [50] D. Li, R. Shao, H. Wang, H. Guo, X. Eric, and H. Zhang, "Mpcformer: fast, performant and private transformer inference with mpc," *International Conference on Learning Representations (ICLR)*, 2023.
- [51] W. Zeng, M. Li, W. Xiong, T. Tong, W.-j. Lu, J. Tan, R. Wang, and R. Huang, "Mpcvit: Searching for accurate and efficient mpc-friendly vision transformer with heterogeneous attention," in *Proceedings of the IEEE/CVF International Conference on Computer Vision*, 2023, pp. 5052–5063.
- [52] K. T. Chitty-Venkata and A. K. Somani, "Neural architecture search survey: A hardware perspective," *ACM Computing Surveys*, vol. 55, no. 4, pp. 1–36, 2022.
- [53] Y. Chang, X. Wang, J. Wang, Y. Wu, L. Yang, K. Zhu, H. Chen, X. Yi, C. Wang, Y. Wang *et al.*, "A survey on evaluation of large language models," *ACM Transactions on Intelligent Systems and Technology*, vol. 15, no. 3, pp. 1–45, 2024.
- [54] S. Domínguez-Almendros, N. Benítez-Parejo, and A. R. Gonzalez-Ramirez, "Logistic regression models," *Allergologia et immunopathologia*, vol. 39, no. 5, pp. 295–305, 2011.
- [55] Y. Yu, X. Si, C. Hu, and J. Zhang, "A review of recurrent neural networks: Lstm cells and network architectures," *Neural computation*, vol. 31, no. 7, pp. 1235–1270, 2019.
- [56] A. Sherstinsky, "Fundamentals of recurrent neural network (rnn) and long short-term memory (lstm) network," *Physica D: Nonlinear Phenomena*, vol. 404, p. 132306, 2020.
- [57] P. Paillier, "Public-key cryptosystems based on composite degree residuosity classes," in *International conference on the theory and applications of cryptographic techniques*. Springer, 1999, pp. 223–238.
- [58] B. Gong, W. F. Lau, M. H. Au, R. Yang, H. Xue, and L. Li, "Efficient zero-knowledge arguments for paillier cryptosystem," in *2024 IEEE Symposium on Security and Privacy (SP)*. IEEE Computer Society, 2024, pp. 93–93.
- [59] T. ElGamal, "A public key cryptosystem and a signature scheme based on discrete logarithms," *IEEE transactions on information theory*, vol. 31, no. 4, pp. 469–472, 1985.
- [60] G. Raju and R. Akbani, "Elliptic curve cryptosystem and its applications," in *SMC'03 Conference Proceedings. 2003 IEEE International Conference on Systems, Man and Cybernetics. Conference Theme-System Security and Assurance (Cat. No. 03CH37483)*, vol. 2. IEEE, 2003, pp. 1540–1543.
- [61] A. S. Reegan and V. Kabila, "Highly secured cluster based wsn using novel fcm and enhanced ecc-elgamal encryption in iot," *Wireless Personal Communications*, vol. 118, no. 2, pp. 1313–1329, 2021.

VIII. SECURITY AGAINST THE SEMI-HONEST ADVERSARY

A. 2PC functionality

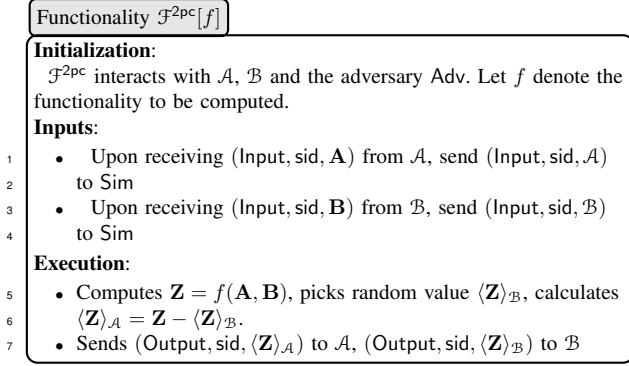


Fig. 12: Functionality for 2PC.

B. Security of Matmul

We define the functionality of Matmul (denoted as $\mathcal{F}_{\text{matmul}}^{2pc}$) as an instance of \mathcal{F}^{2pc} , where $\mathcal{F}_{\text{matmul}}^{2pc}$ calculates $\mathbf{Z} = f(\mathbf{A}, \mathbf{B}) := \mathbf{A} \otimes \mathbf{B}$. If \mathcal{B} is the corrupted party, instead of picking random $\langle \mathbf{Z} \rangle_{\mathcal{B}}$, $\mathcal{F}_{\text{matmul}}^{2pc}$ receives (Modify, sid, $\langle \mathbf{Z} \rangle_{\mathcal{B}}$) from Sim, calculates $\langle \mathbf{Z} \rangle_{\mathcal{A}} = \mathbf{Z} - \langle \mathbf{Z} \rangle_{\mathcal{B}}$.

Theorem 1. *The protocol Π_{matmul} is securely computes functionality $\mathcal{F}_{\text{matmul}}^{2pc}$ in the presence of static semi-honest adversaries Adv controlling each of parity \mathcal{A} or \mathcal{B} .*

Proof. Consider the first case that \mathcal{A} is corrupted. In the protocol, \mathcal{A} receives a single message $[\langle \mathbf{C} \rangle_{\mathcal{A}}]_{\mathcal{A}}$. We construct the simulator Sim as follows:

- Sim sends (Input, sid, \mathbf{A}) to $\mathcal{F}_{\text{matmul}}^{2pc}$.
- Sim receive $[\langle \tilde{\mathbf{A}} \rangle_{\mathcal{A}}]_{\mathcal{A}}$ from the corrupted party \mathcal{A} .
- Upon receiving $\langle \mathbf{Z} \rangle_{\mathcal{A}}$ from $\mathcal{F}_{\text{matmul}}^{2pc}$, Sim encrypt it as $\mathbf{c} = [\langle \mathbf{Z} \rangle_{\mathcal{A}}]_{\mathcal{A}}$ and forward \mathbf{c} to corrupted \mathcal{A}

Indistinguishable. Obviously, when the corrupted \mathcal{A} receives $\mathbf{c} = [\langle \mathbf{Z} \rangle_{\mathcal{A}}]_{\mathcal{A}}$, it will decrypt it and set $\langle \mathbf{Z} \rangle_{\mathcal{A}}$ as result, leading a correct output. For the incoming message $[\langle \mathbf{C} \rangle_{\mathcal{A}}]_{\mathcal{A}}$ of the corrupted \mathcal{A} , due to that $\langle \mathbf{C} \rangle_{\mathcal{A}}$ is encrypted with one-time pad, with the random key \mathbf{R} , \mathcal{A} cannot distinguish it from the random value $\langle \mathbf{Z} \rangle_{\mathcal{A}}$ of the ideal world.

Consider the second case that \mathcal{B} is corrupted. In the protocol, \mathcal{B} receives a single message $[\tilde{\mathbf{A}}_i]_{\mathcal{A}}$. We construct the simulator Sim as follows:

- Sim sends (Input, sid, \mathbf{B}) to functionality $\mathcal{F}_{\text{matmul}}^{2pc}$.
- Sim picks random value \mathbf{A}' and sends $[\tilde{\mathbf{A}}']_{\mathcal{A}}$ to corrupted \mathcal{B} ;
- Upon receiving $[\langle \mathbf{C} \rangle_{\mathcal{A}}]_{\mathcal{A}}$ from corrupted \mathcal{B} , Sim extracts \mathbf{R} as $\mathbf{R} = \langle \mathbf{C} \rangle_{\mathcal{A}} - \mathbf{A}'/\mathbf{B}$;
- Sim sends (Modify, sid, \mathbf{R}) to functionality $\mathcal{F}_{\text{matmul}}^{2pc}$.

Indistinguishable. Obviously, when the corrupted \mathcal{B} sets its output as \mathbf{R} , $\mathcal{F}_{\text{matmul}}^{2pc}$ will output $\mathbf{A}\mathbf{B} - \mathbf{R}$ to \mathcal{A} , leading a correct output. For the incoming message $[\tilde{\mathbf{A}}_i]_{\mathcal{A}}$ of the corrupted \mathcal{B} ,

if the adversary Adv can distinguish $[\tilde{\mathbf{A}}'_i]_{\mathcal{A}}$ and $[\tilde{\mathbf{A}}_i]_{\mathcal{A}}$, we can construct a game to break the BFV scheme.

C. Security of SoftMax

We define the functionality of SoftMax (denoted as $\mathcal{F}_{\text{softmax}}^{2pc}$) as an instance of \mathcal{F}^{2pc} , where $\mathcal{F}_{\text{softmax}}^{2pc}$ calculates $\mathbf{Z} = f(\langle \mathbf{X} \rangle_{\mathcal{A}}, \langle \mathbf{X} \rangle_{\mathcal{B}}) := \text{SoftMax}(\frac{e^{x_i}}{\sum_{j=0}^{m-1} e^{x_{ij}}})$. if \mathcal{A} is the corrupted party, instead of picking randoms $\langle \mathbf{Z} \rangle_{\mathcal{A}}$, $\mathcal{F}_{\text{softmax}}^{2pc}$ receives (Modify, sid, $\langle \mathbf{Z} \rangle_{\mathcal{A}}$) from Sim, calculates $\langle \mathbf{Z} \rangle_{\mathcal{B}} = \mathbf{Z} - \langle \mathbf{Z} \rangle_{\mathcal{A}}$.

Theorem 2. *The protocol Π_{softmax} is securely computes functionality $\mathcal{F}_{\text{softmax}}^{2pc}$ in the presence of static semi-honest adversaries Adv controlling each of parity \mathcal{A} or \mathcal{B} .*

Proof. Consider the first case that \mathcal{A} is corrupted. In the protocol, \mathcal{A} receives messages $[\langle \mathbf{E} \rangle_{\mathcal{B}}]_{\mathcal{B}}$, $[\sum(\mathbf{E}) \odot \mathbf{v}]_{\mathcal{A}}$, $[\widehat{\mathbf{V}}]_{\mathcal{B}}$. We construct the simulator Sim as follows:

- Sim sends (Input, sid, $\langle \mathbf{X} \rangle_{\mathcal{A}}$) to $\mathcal{F}_{\text{softmax}}^{2pc}$.
- Sim picks random values $\langle \mathbf{E} \rangle'_{\mathcal{B}}$, $\widehat{\mathbf{V}}'$ and sends $[\langle \mathbf{E} \rangle']_{\mathcal{B}}$, $[\widehat{\mathbf{V}}']_{\mathcal{B}}$ to corrupted party \mathcal{A} .
- Upon receiving $[\tilde{\mathbf{E}} \oplus \mathbf{R}]_{\mathcal{B}}$, $[\mathbf{SR}]_{\mathcal{A}}$, $[\langle \mathbf{Y} \rangle_{\mathcal{B}}]_{\mathcal{B}}$ from corrupted \mathcal{A} . Sim can extract $\tilde{\mathbf{E}} \oplus \mathbf{R}$, and \mathbf{M}
- Sim sends (Modify, Sid, $\tilde{\mathbf{E}} \oplus \mathbf{R}$, (Modify, Sid, \mathbf{M}) to functionality $\mathcal{F}_{\text{softmax}}^{2pc}$.

Indistinguishable. Obviously, when the corrupted \mathcal{A} sets its output as \mathbf{M} , $\mathcal{F}_{\text{softmax}}^{2pc}$ will output $\mathbf{Z} - \mathbf{M}$ to \mathcal{A} , leading a correct output. For the incoming messages $[\langle \mathbf{E} \rangle_{\mathcal{B}}]_{\mathcal{B}}$, $[\widehat{\mathbf{V}}]_{\mathcal{B}}$ of the corrupted \mathcal{A} , if the adversary Adv can distinguish $[\langle \mathbf{E} \rangle']_{\mathcal{B}}$, $[\widehat{\mathbf{V}}']_{\mathcal{B}}$, we can construct a game to break the BFV scheme. And with random key \mathbf{v} , \mathcal{A} can not distinguish it from the random value $\sum(\mathbf{E}) \odot \mathbf{v}$ of the ideal world.

Consider the second case that \mathcal{B} is corrupted. In the protocol, \mathcal{B} receives messages $[\tilde{\mathbf{E}} \oplus \mathbf{R}]_{\mathcal{B}}$, $[\mathbf{SR}]_{\mathcal{A}}$, $[\langle \mathbf{Y} \rangle_{\mathcal{B}}]_{\mathcal{B}}$. We construct the simulator Sim as follows:

- Sim sends (Input, sid, \mathbf{B}) to functionality $\mathcal{F}_{\text{softmax}}^{2pc}$.
- Sim receives $[\langle \mathbf{E} \rangle_{\mathcal{B}}]_{\mathcal{B}}$, $[\widehat{\mathbf{V}}]_{\mathcal{B}}$ from the corrupted party \mathcal{B} .
- Sim picks random value \mathbf{SR}' and sends $[\mathbf{SR}']_{\mathcal{A}}$ to corrupted \mathcal{B} ;
- Upon receiving $[\sum(\mathbf{E}) \odot \mathbf{v}]_{\mathcal{A}}$, from the corrupted \mathcal{B} , Sim extracts $\sum(\mathbf{E}) \odot \mathbf{v}$,
- Sim sends (Modify, sid, $\sum(\mathbf{E}) \odot \mathbf{v}$) to functionality $\mathcal{F}_{\text{softmax}}^{2pc}$.

Indistinguishable. Obviously, when the corrupted \mathcal{B} receives $\mathbf{c} = \langle \mathbf{Y} \rangle_{\mathcal{B}}$, it will decrypt it and set $\langle \mathbf{Y} \rangle_{\mathcal{B}}$ as a result, leading a correct output. For the incoming message $[\tilde{\mathbf{E}} \oplus \mathbf{R}]_{\mathcal{B}}$, $[\langle \mathbf{Y} \rangle_{\mathcal{B}}]_{\mathcal{B}}$ of the corrupted \mathcal{B} , due that $\tilde{\mathbf{E}} \oplus \mathbf{R}$ and $\langle \mathbf{Y} \rangle_{\mathcal{B}}$ is encrypted with one-time pad, with the random key \mathbf{R} and \mathbf{M} , \mathcal{B} cannot distinguish it from the random value $\langle \mathbf{Z} \rangle_{\mathcal{B}}$ and $\tilde{\mathbf{E}}$ of the ideal world. For the incoming $[\mathbf{SR}]_{\mathcal{A}}$ of corrupted \mathcal{B} , if the adversary Adv can distinguish $[\mathbf{SR}]_{\mathcal{A}}$ and $[\mathbf{SR}']_{\mathcal{A}}$, we can construct a game to break the BFV scheme.

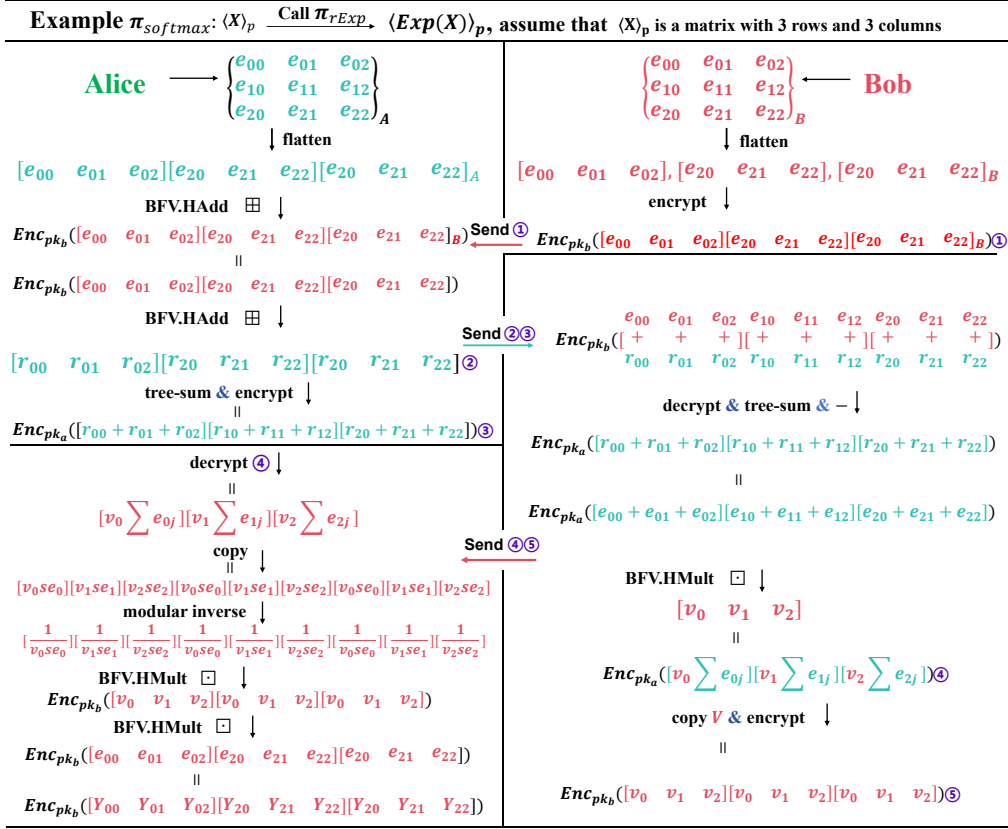


Fig. 13: The example of Π_{softmax}

D. Security of LayerNorm

We define the functionality of LayerNorm (denoted as $\mathcal{F}_{\text{In}}^{2\text{pc}}$) as an instance of $\mathcal{F}^{2\text{pc}}$, where $\mathcal{F}_{\text{In}}^{2\text{pc}}$ calculates $\mathbf{Z} = f(\langle \mathbf{X} \rangle_A, \langle \mathbf{X} \rangle_B) := \text{LayerNorm}(\gamma \cdot \frac{x_i - \mu}{\sigma} + \beta)$. if \mathcal{B} is the corrupted party, instead of picking randoms $\langle \mathbf{Z} \rangle_B$, $\mathcal{F}_{\text{In}}^{2\text{pc}}$ receives (Modify, sid, $\langle \mathbf{Z} \rangle_B$) from Sim, calculates $\langle \mathbf{Z} \rangle_A = \mathbf{Z} - \langle \mathbf{Z} \rangle_B$.

Theorem 3. *The protocol Π_{In} is securely computes functionality $\mathcal{F}_{\text{In}}^{2\text{pc}}$ in the presence of static semi-honest adversaries Adv controlling each of parity A or B .*

Proof. The proof process is the same as that of SoftMax.

IX. SEGMENTAL APPROXIMATION OF NONLINEAR FUNCTIONS

A. Approximation of GeLU

The piecewise polynomial approximations F1 and F2 for the seg5GeLU function are as follows:

$$\begin{aligned}
 F_1(x) &= -0.568686678 - 0.529288810x - 0.183509590x^2 \\
 &\quad - 0.028070202x^3 - 0.001597741x^4 \\
 F_2(x) &= 0.001193207 + 0.5x + 0.385858026x^2 - 0.045101361x^4 \quad (31) \\
 F_3(x) &= -0.438406187 + 1.340789252x - 0.087184212x^2 \\
 &\quad + 0.007334718x^3
 \end{aligned}$$

B. Approximation of Sigmoid

The Sigmoid function is:

$$y = \text{Sigmoid}(x) = \frac{1}{1 + e^{-x}} \quad (32)$$

which is regarding (0, 0.5) symmetry, so we can just concern the situation where $x \geq 0$, and for $x < 0$, $\text{Sigmoid}(x) = 1 - \text{Sigmoid}(-x)$. Its derivatives is $y' = y(1 - y) > 0$, so we can get its second derivative: $y'' = y'(1 - 2y)$; And its third derivative: $y''' = y'(6y^2 - 6y + 1)$. Let $y'' = 0$, we can get $x = 0$, and let $y''' = 0$, due to $y' > 0$, so let $6y^2 - 6y + 1 = 0$, that is $y = \frac{3 \pm \sqrt{3}}{6}$, and we obtain the inflection point $x_1 = \ln(2 \pm \sqrt{3})$. Because of $x \geq 0$, so $x_1 = \ln(2 + \sqrt{3})$. We can obtain the other inflection point $x_2 = 6.48$, when $y'' < 10^{-5}$. Consequently, we can derive a piecewise approximation to the Sigmoid function:

$$\text{seg4Sigmoid}(x) = \begin{cases} F_1(x), & \text{if } 0 \leq x < x_1 \\ F_2(x), & \text{if } x_1 \leq 0 < x_2 \\ 1, & \text{if } x \geq x_2 \end{cases} \quad (33)$$

where the interval functions F_1 and F_2 are given below:

$$\begin{aligned} F_1(x) &= 0.4998102695 + 0.2527736008x - 0.0086980795^2 \\ -0.0127621849x^3 \quad F_2(x) &= 0.4489827105 + 0.3642809155 - 0.0948498277x^2 \\ &\quad + 0.0113621587x^3 - 0.0005220290x^4 \end{aligned} \quad (34)$$

Seg4Sigmoid for the negative half-axis can be easily obtained based on the symmetry.

C. Approximation of Tanh

Tanh's graphics is similar to Sigmoid's, the Tanh function is:

$$y = \tanh(x) = \frac{e^x - e^{-x}}{e^x + e^{-x}} \quad (35)$$

Tanh is regarding $(0,0)$ symmetry, similar to Sigmoid, we can just concern the situation where $x \geq 0$, and for $x < 0$, $\tanh(x) = -\tanh(-x)$. Its derivative is $y' = 1 - y^2 > 0$, so we can get its second derivative: $y'' = 2yy'$; And its third derivative: $y''' = 2y'(3y^2 - 1)$. Let $y'' = 0$, we can get $x = 0$, and let $y''' = 0$, due to $y' > 0$, so $3y^2 - 1 = 0$, that is $y = \pm \frac{1}{\sqrt{3}}$, and we obtain the point $x_1 = \ln \frac{\sqrt{3}+1}{\sqrt{2}}$. Because of $x \geq 0$, so $x_1 = \ln \frac{\sqrt{3}+1}{\sqrt{2}}$. We can locate the segmentation point $x'_1 = \ln \frac{\sqrt{3}+2}{\sqrt{2}}$ on either side of x_1 which results in the smallest error. We can also obtain the other inflection point $x_2 = 4.60$ when $y'' < 10^{-5}$. Consequently, we can derive a piecewise approximation to the Tanh function:

$$\text{seg4Tanh}(x) = \begin{cases} F_1(x), & \text{if } 0 \leq x < x'_1 \\ F_2(x), & \text{if } x'_1 \leq 0 < x_2 \\ 1, & \text{if } x \geq x_2 \end{cases} \quad (36)$$

where the interval functions F_1 and F_2 are given below:

$$\begin{aligned} F_1(x) &= -0.0018890324 + 1.0384417257x - 0.1695016932x^2 \\ &\quad - 0.1084776546x^3 \\ F_2(x) &= 0.0800126966 + 1.0756763251x - 0.4766182792x^2 \\ &\quad + 0.0938427835x^3 - 0.0068823466x^4 \end{aligned} \quad (37)$$

Compared with Bolt, which employs a piecewise polynomial of degree 5, our model, using a fourth-degree polynomial, still achieves higher fitting accuracy.

D. Approximation of Mish

Mish's graphics is similar to GeLU's, but it has no symmetry with its derivative. The Mish function is:

$$y = \text{Mish}(x) = x \tanh(\ln(1 + e^x)) \quad (38)$$

Because y'' and y''' are too complex and hard to get their zero point, we use dichotomy to get y''' 's approximate zero point: $x_1 = -2.2563763963607935$ and $x_2 = 1.4905711794854284$. Consequently, we can derive a piecewise approximation to the Mish function:

$$\text{seg4Mish}(x) = \begin{cases} 0, & \text{if } x < -8 \\ F_1(x), & \text{if } -8 \leq x < x_1 \\ F_2(x), & \text{if } x_1 \leq x < x_2 \\ F_3(x), & \text{if } x_2 \leq x < 8 \\ x, & \text{if } x \geq 8 \end{cases} \quad (39)$$

where the interval functions F_1 , F_2 and F_3 are given below:

$$\begin{aligned} F_1(x) &= -0.1150272397 + 0.5194677655x + 0.4293028981x^2 \\ &\quad + 0.1459472737x^3 + 0.0271015218x^4 + 0.0028988426x^5 \\ &\quad + 0.0001685503x^6 + 0.0000041415x^7 \\ F_2(x) &= 0.0000929623 + 0.5993108159x + 0.3185423599x^2 \\ &\quad - 0.0135480666x^3 - 0.0420248186x^4 - 0.0022342097x^5 \\ &\quad + 0.0043057993x^6 + 0.0008690923x^7 \\ F_3(x) &= -0.2470775212 + 1.0311064672x + 0.1227243900x^2 \\ &\quad - 0.0757410810x^3 + 0.0200857395x^4 - 0.0027959123x^5 \\ &\quad + 0.0002003775x^6 - 0.000005848x^7 \end{aligned} \quad (40)$$

E. Example of the secure Softmax Π_{softmax} & Π_{ln}

Here are two examples, with Fig. 13 and Fig. 14 corresponding to Π_{softmax} and Π_{ln} , respectively.

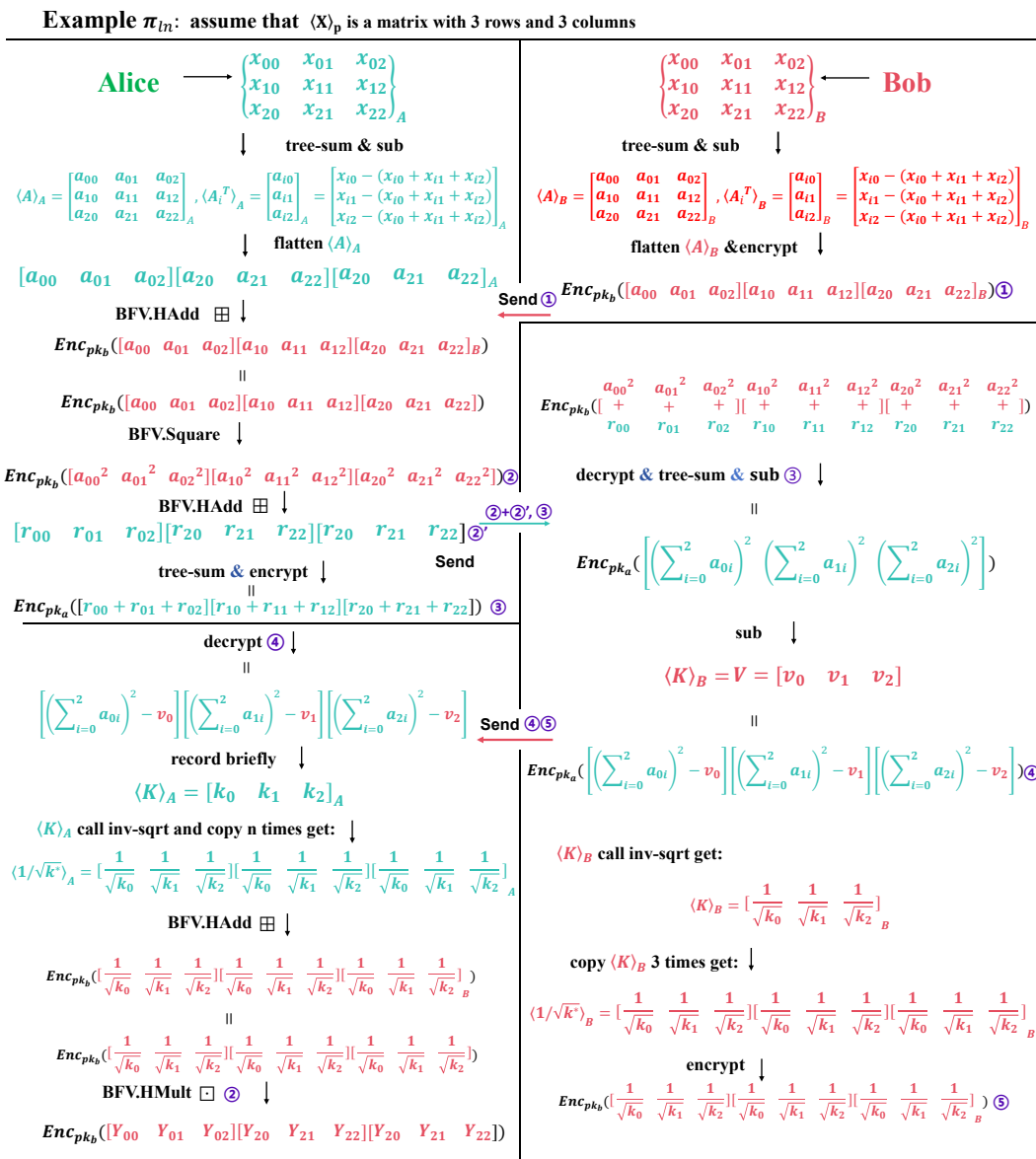


Fig. 14: The example of Π_{In}